Liquid Phase Sintering

In two phase systems involving mixed powders, it is possible to form a low melting phase. In such a system, the liquid may provide for rapid transport and therefore rapid sintering if certain criteria are met.

Wetting is the first requirement, as the liquid must form a film around the solid phase. A wetting liquid has a small contact angle θ, defined by the equilibrium of surface energies;

$$\gamma_{SV} = \gamma_{SL} + \gamma_{LV}\cos(\theta)$$

where γ_{SV} is the solid-vapor surface energy, γ_{SL} is solid-liq. and γ_{LV} liq-vapor.

A small contact angle indicates the liquid will spread over the solid surface. The solid must be soluble in the liquid. Finally, the diffusive transport for the dissolved solid atoms should be high enough to ensure rapid sintering.

Densification

In liquid phase sintering, once the liquid forms it will flow to wet the particles. Figure is a densification schematic for liq. phase sintering. Initially, particle rearrangement contributes to densification. With continued heating, the solid phase dissolves into the liquid and the amount of liq. grows until it saturated with the solid component. The liq. phase then becomes a carrier for the solid phase atoms in a process termed solution–reprecipitation, wherein the small grains dissolve and reprecipitate on the large grains.

The solubility of a solid grain varies inversely with the grain size. Small grains preferentially dissolve in the liquid phase and over time, the grain number decreases while the grain size increases.

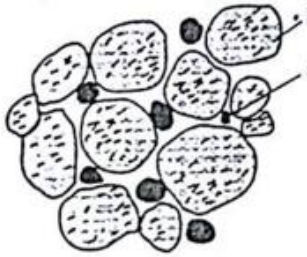

green

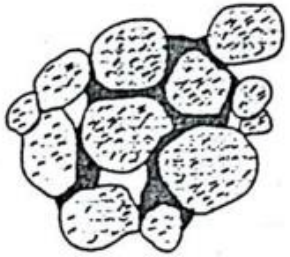
liquid spreading

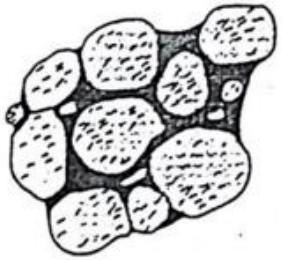
solution reprecipitation

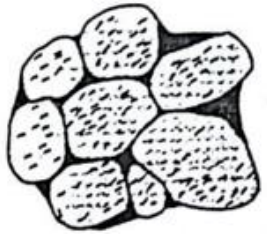
solid skeleton

Figure shows the solution_reppt process with grain shape accomodation.

Depending on the volume fraction of liquid and the dihedral angle, several different grain–liq. structures are possible. Typically, the dihedral angle is small, on the order of 20 to 40° and the volume of liq. is below 15 vol%.

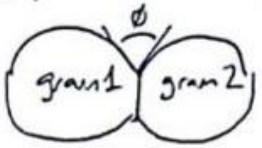

As volume fraction of liq. increases, the ease of densification also increases, but compact slumping (shearing) becomes a problem. Figure shows a schematic of densification vs. liq. content

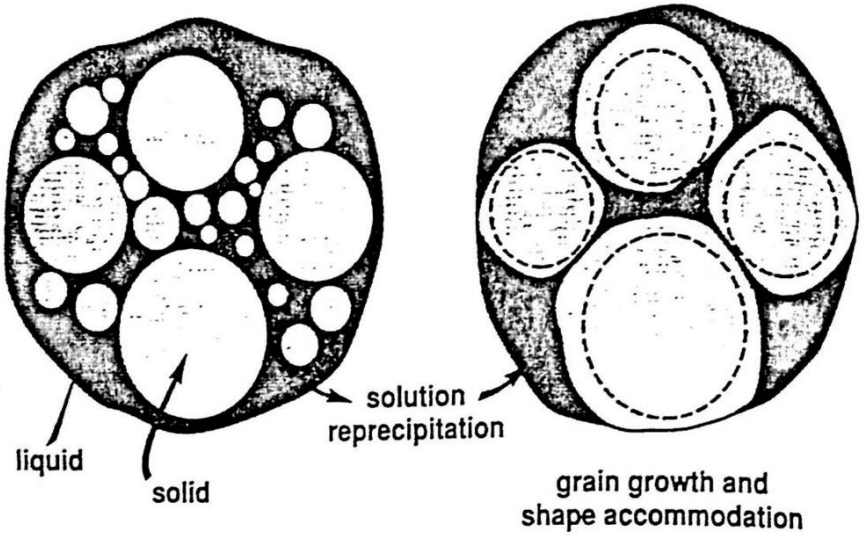

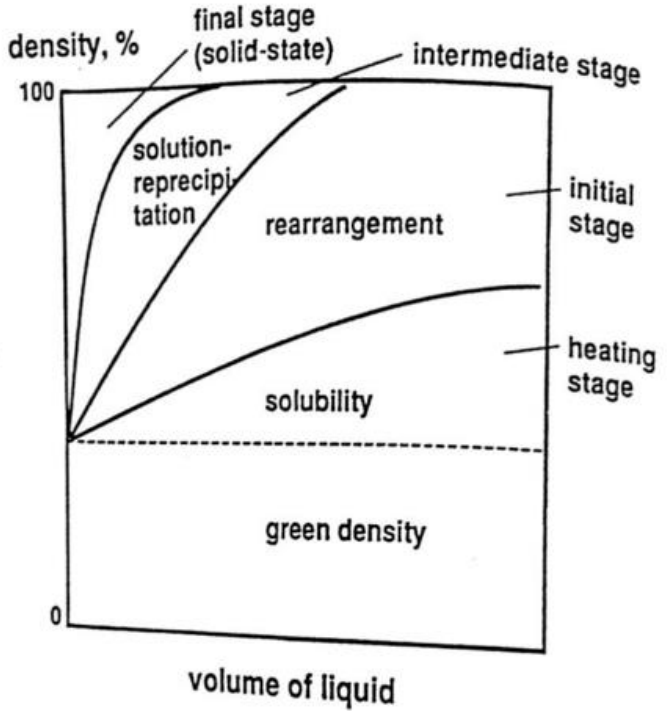

If there is no liquid, then sintering is by solid-state processes. On the other hand, with an excess of liquid (over approx 35 vol%) all pores btw particles is filled as soon as the liquid forms; however, the mixture may be too fluid to hold compact shape.

Coarsening

During liq. phase sintering, the solid phase will coarsen at a rate such that average grain size G enlarges with either the one-half or one-third power of time.

Full Density Processing

In the ideal, a component is fabricated with final dimensions requiring no post-consolidation machining. That goal is termed "net shaping," and full density is one of the best approaches.

Eliminating residual pores while obtaining the desired final dimensions is the challenge. With prolonged sintering, the pore structure becomes stabilized and is difficult to remove from a compact via diffusion. However, the properties of many materials can be improved. The ability to control microstructure, segregation, grain size, inclusion population, and the material texture has motivated considerable exploration of full density PM processing.

A basic conflict of full density processing is that the actions necessary for densification are those which also add the greatest expense. The conflict between performance and cost may be resolved in many ways. The best approach is to determine the properties needed in a situation and then decide on the density necessary for the level of performance.

Some of the options between performance and porosity are shown in Figure. Although not comprehensive, various processes are located on the performance vs. density plot in terms of compact size.

Although the figure is schematic, it provides a first view of full density processing which stimulates 4 questions: First, are the properties actually needed? Second, what are the limitations in terms of materials, processes, properties, and size? Third, can the cost of the processing options be justified? Finally, would changes in the material, technology, or density be most appropriate?

Generally increased performance implies a higher density. For smaller components and moderate performance levels, traditional press and sinter technology is most useful. As the component shape complexity increases, then PIM becomes a better alternative.

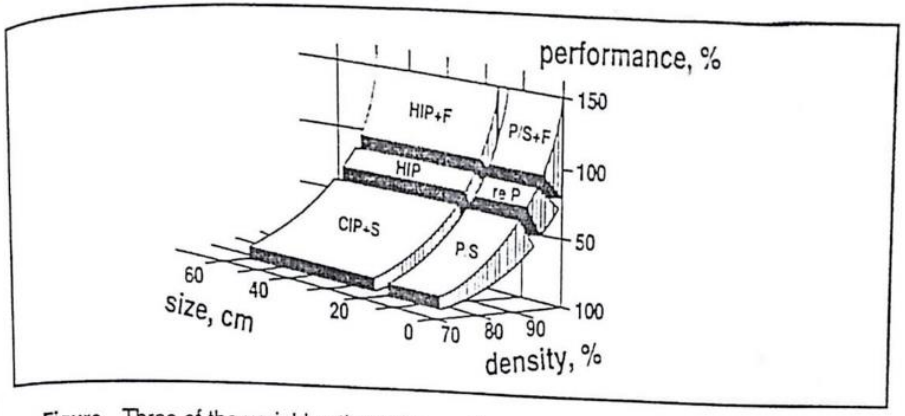

Figure Three of the variables that influence the selection of a powder metallurgy processing methods - component size, density, and performance (as a percentage of wrought). That behavior corresponds to ferrous based P/M systems formed from coarse powder, but is representative of many powder metallurgy materials. The symbols are P/S = press and sinter; reP = press, sinter and repress; P/S+F = press, sinter and forge; CIP+S = cold isostatically press and sinter; HIP = hot isostatically press; HIP+F = hot isostatically press and forge.

Advantages and Disadvantages of Full Density Processing

In most instances, the performance of materials improves with a higher density. Attaining full density is difficult. Therefore, full density provides on the one hand improved properties, on the other hand it represents high level of difficulty and expense over traditional pressing and sintering processes.

More specialized equipment is often required to obtain full densities. Additionally, dimensional control can be lost with some of the techiques. The type of powder most responsive to full density processing is a clean, prealloyed powder usually a specialited input material.

Another advantage of full density powder product is the wide range of shapes, sizes and materials available.

Consolidation Fundamentals

Infiltration and enhanced sintering treatments are full density processing methods which do not require external stress. Many full density methods do employ various combinations of temperature and stress. The traditional cycle involves sequential compaction or shaping at low temperatures followed by sintering as a second operation. Hot consolidation of powder combines the compaction and sintering steps into one operation.

The simultaneous heating and pressurization events add cost and complexity that are best justified by increased performance

Full density processing is normally ineffective at temperatures below approx. one half of the absolute melting T. Temperatures btw 70 and 85% of T_M are typical.

Hot Consolidation Techniques

Uniaxial Hot Pressing: Hot pressing can be performed in a rigid die using uniaxial pressurization as shown in figure. Note the features are similar to die compaction. The die is usually made from graphite to allow external induction heating. Other common die materials are refractory metals and their alloys, and sometimes ceramics such as silicon carbide can be used at low stresses.

If the compact exhibits an incompatible thermal expansion coefficient, then cracking may occur during cooling. In such cases it is appropriate to eject the compact at high temperature.

Uniaxial hot pressing is slow and inherently has poor control over the heating and cooling stages because of the large thermal mass associated with tooling. Typical max T_s are 2200°C and max pressures are 50 MPa. Vacuum is often selected for the process environment to minimize contamination of the compact.

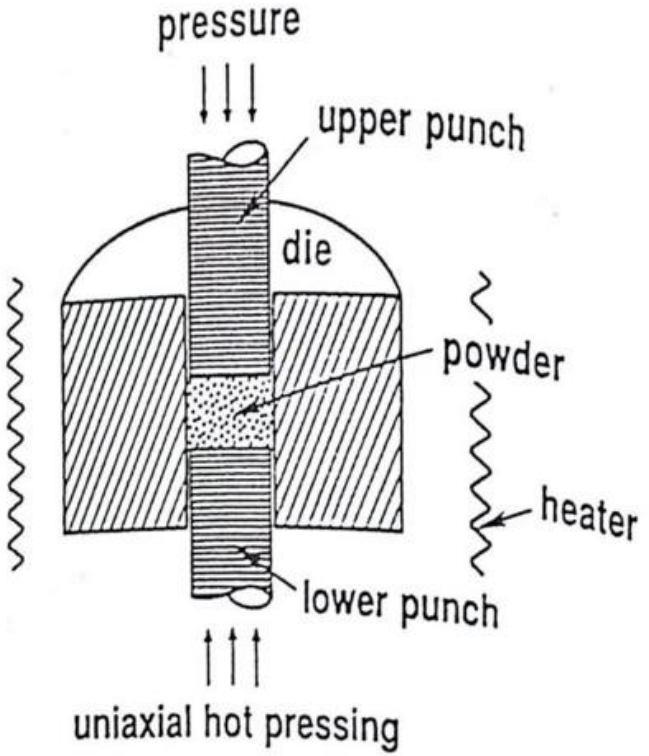

The dies and apparatus can be expensive, especially if pressing is performed under vacuum. Contamination of the compact from the die is a common problem. However, uniaxial hot pressing is widely used to fabricate unique compositions and composites. One large commercial use for uniaxial pressing is in the consolidation of diamond–metal composite cutting tools.

Hot Isostatic Compaction: Flexible dies are used in hot isostatic pressing with isotropic pressurization. The primary control parameters are pressure (stress), temperature and time. Figure shows a schematic of the hot isostatic pressing (HIP) sequence. For loose powder, a gas-tight container is used to shape the powder. The container may be fabricated from any material that is deformable at the consolidation temp. Prior to HIP consolidation, the filled container is heated and vacuum degassed to remove volatile contaminants. After prolonged evacuation and degassing, the container is sealed.

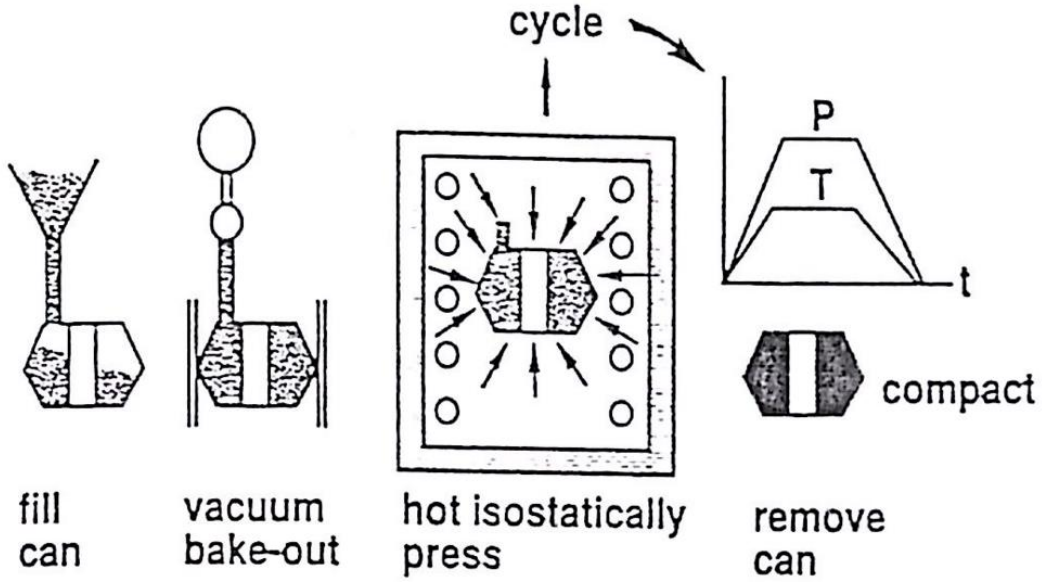

One variant is to use previously sintered compacts with densities over 92% of theoretical, which corresponds to the point of pore closure. In that case, the component already has the desired shape and the closed pores allow for HIP. This approach is widely used to consolidate cemented carbides, wear materials, and titanium implants.

An Introduction to Glass Science

DEFINITION

Glass is an amorphous material, and the most important properties can be counted as;

- it is transparent,
- it is inert to reactions with most of the chemicals; and
- it is strong and rigid.
- it is non-porous

The worst property of glass is its fragility.

The most accepted definition of glass is the one suggested by ASTM at 1945:

"Glass- an inorganic product of fusion that has cooled to a rigid condition without crystallization."

Crystalline Silica

If silica (SiO_2) which is a highly viscous liquid, is cooled very slowly, it can form a crystalline solid material called quartz.

In crystalline silica, Silicon ion (Si^{4+}) forms a constraction unit, together with 4 oxygen ions (O^{2-}) around it.

In this construction unit, silicon takes place in the center of the unit and it is surrounded by oxygens to form a tetrahedron.

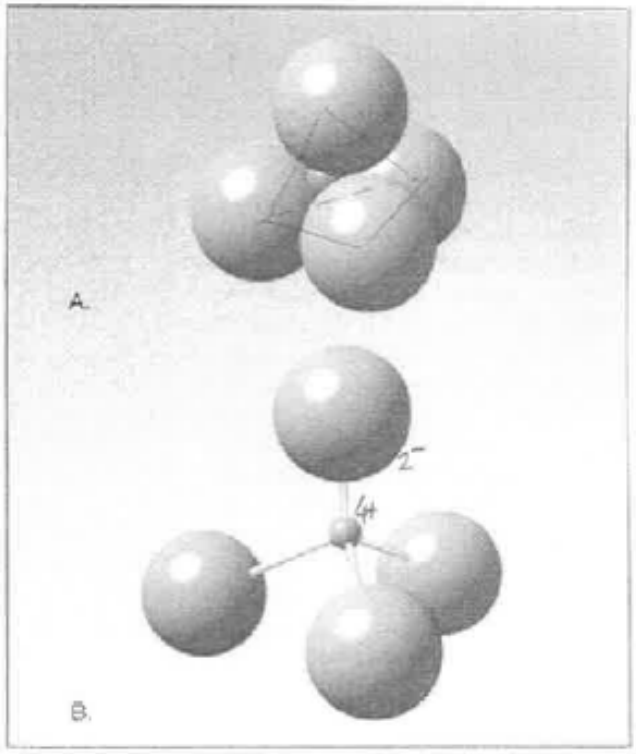

If these tetrahedra can arrange themselves through sufficiently slow cooling, a regular structure will emerge.

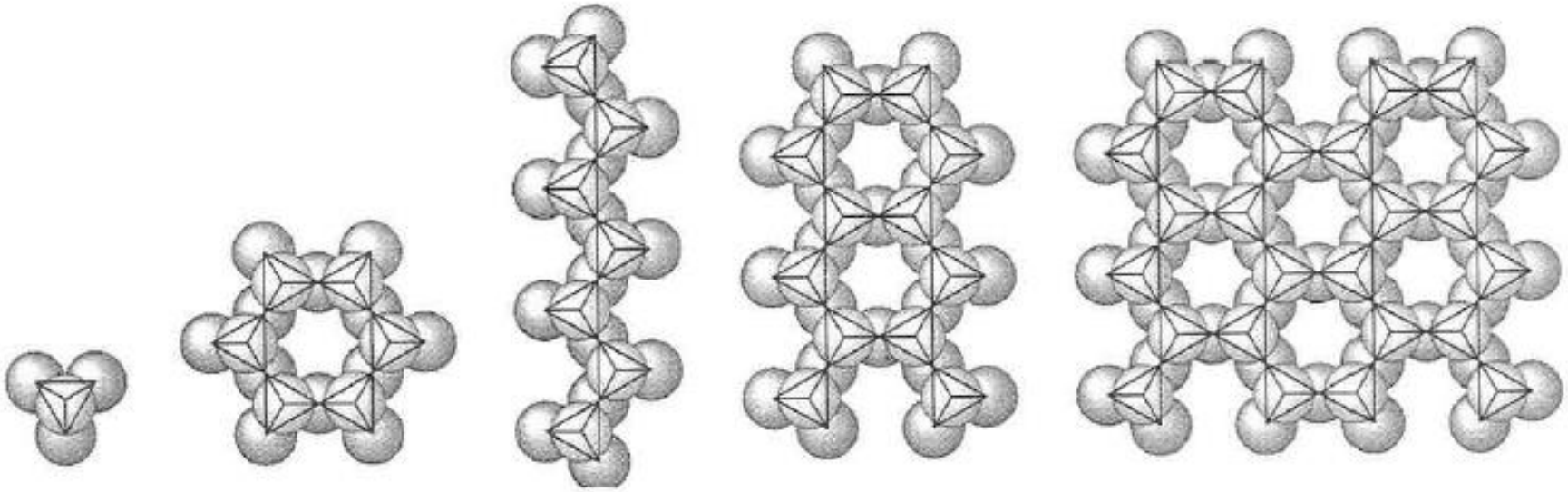

Silica tetrahedron

Crystalline silica (quartz)

Vitreous Silica

When a rapid cooling is applied, silica tetrahedra can not arrange themselves accordingly. In this way, the glass state will develop.

In two dimensional scheme

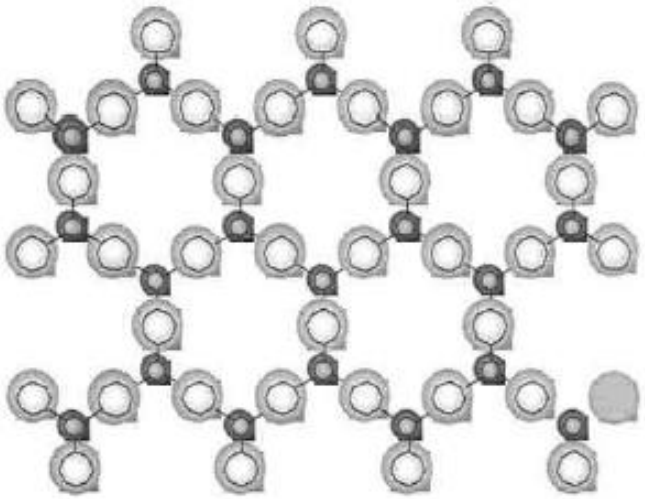

Crystalline silica

(quartz)

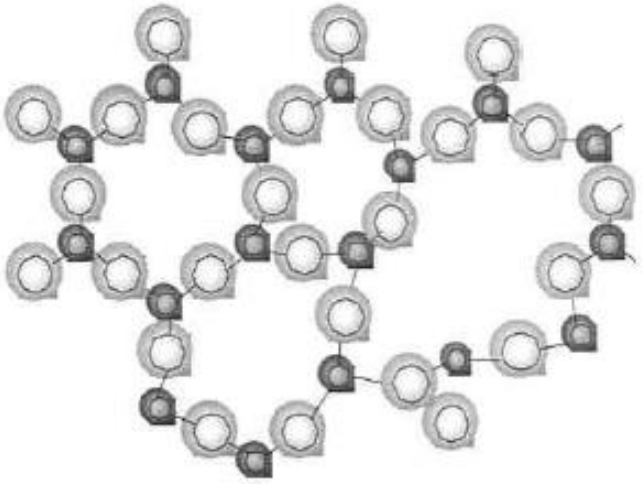

Vitreous silica

Although there are irregular holes between the structural units of vitreous silica, Si-O-Si bonds are very strong bonds.

These oxygens, taking place in the network, are called bridging oxygens.

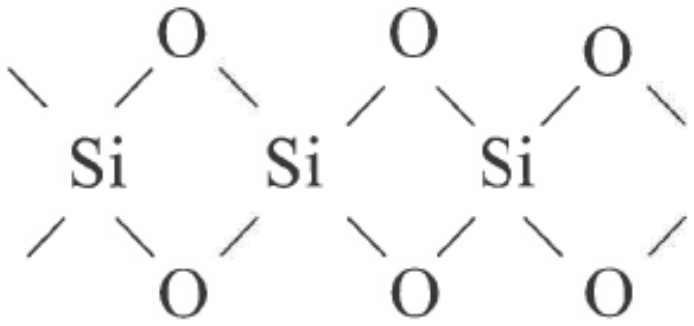

Bridging oxygens

Alkali Metals (Li, Na, K)

(Network Modifiers)

- They are at the first column (IA) of periodic table.
- They have one single electron at their last orbit. So they can easily give this electron and form an ionic bond with the oxygen in the network.
- They break the strong covalent bonds of the network, Si-O-Si (Bridging property) and form weak ionic bonds. Oxygen ions which take place in these ionic bonds called non-bridging oxygens.
- They called as modifiers.

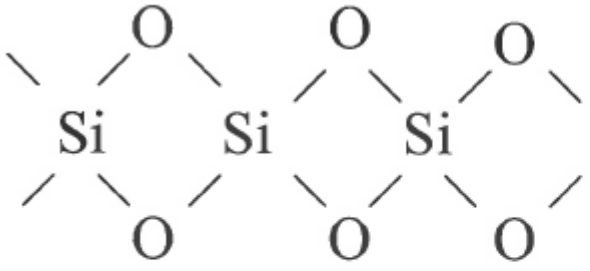

Bridging oxygen

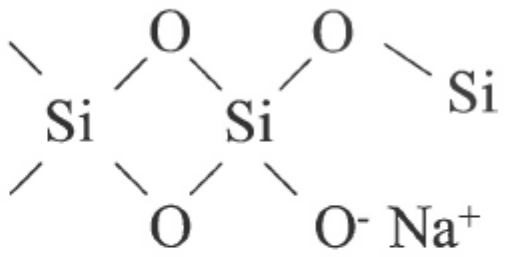

Non-bridging oxygen
(bonded to alkali ion)

Alkali ions (Li, Na, K)

Attraction force

$Li^+ < Na^+ < K^+$

Ionic radius

Alkaline Earth Metals (Mg, Ca, Sr, Ba)

(Network Modifiers)

- They are at the second column (IIA) of periodic table.

- They have two electrons at their last orbit, so they can give these electrons (gain +2 charge) and form two ionic bonds with two oxygens in the network. They are modifiers as well.

- They break the strong covalent bonds of the network like alkali metals, and they form two ionic bonds. Since they are bonded to two non-bridging oxygens, they hang on the network more strongly than alkali ions.

- Like the alkali ions, they break the network continuity.

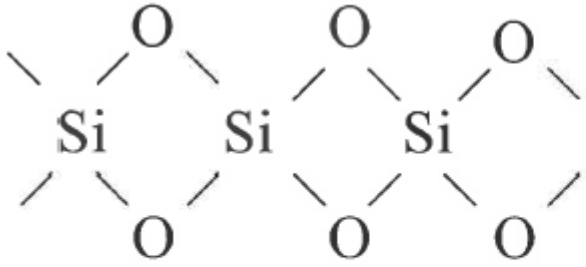

Bridging oxygen

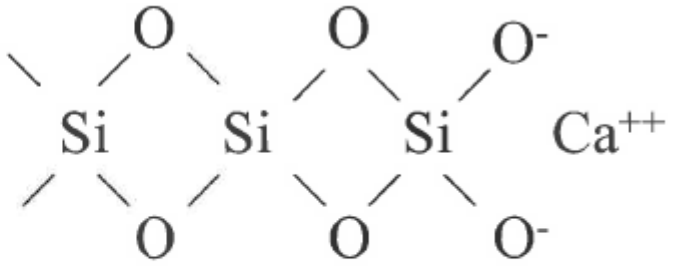

Non-bridging oxygen

(bonded to alkaline earth ion)

Alkaline earth ions (Mg^{2+}, Ca^{2+}, Sr^{2+}, Ba^{2+})

Attraction force

←

Mg < Ca < Sr < Ba

→

Ionic radius

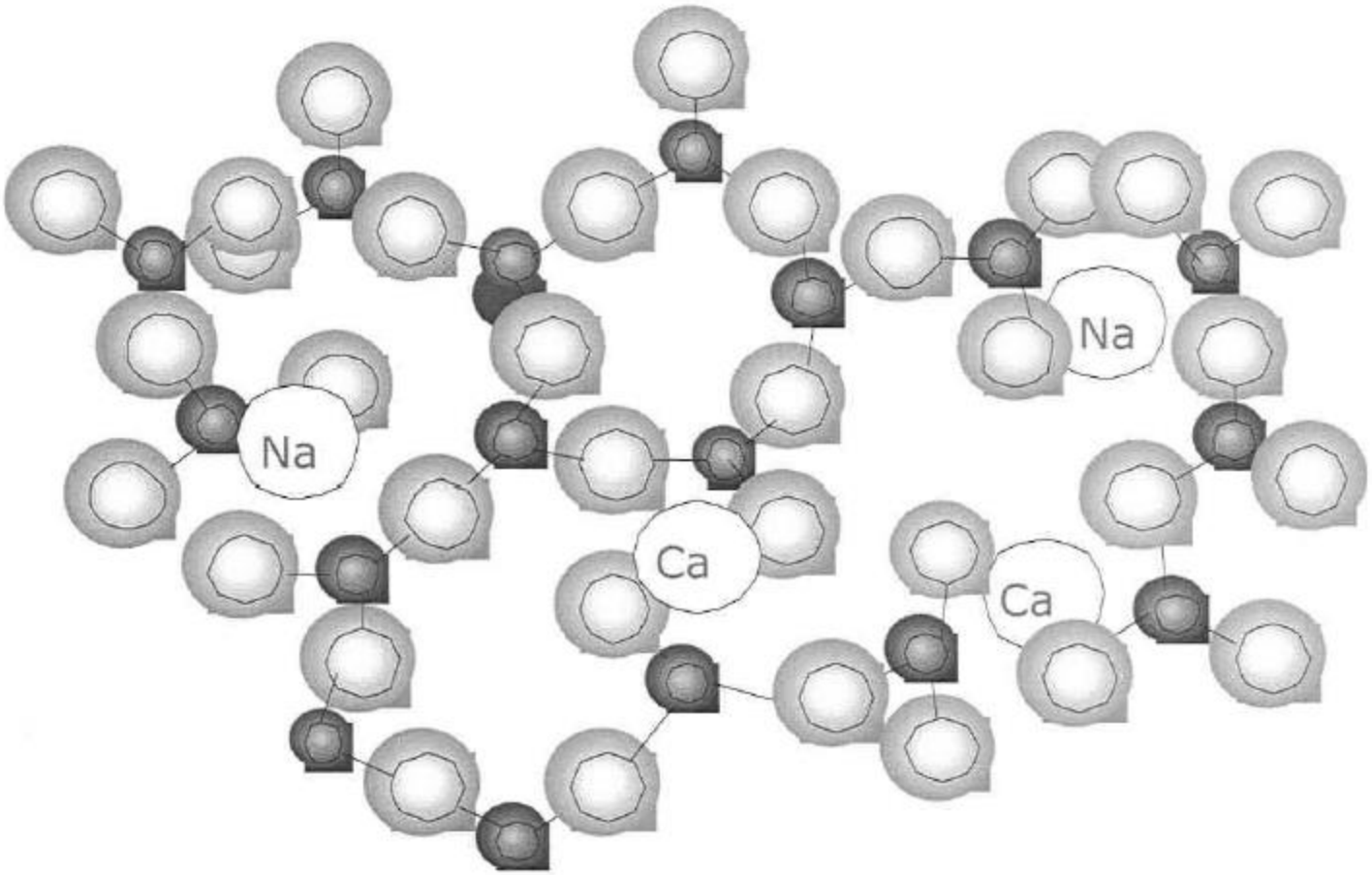

Structure of soda-lime-silicate glass

Aluminum

(Intermediate)

- It stays on the third column (IIIA) of the periodic table.

- It shows both covalent and ionic character (amphoteric). As a result of having small ionic radius and high electronic charge (3+), it forms strong bonds with oxygen.

- Since it is amphotheric it can form AlO_4^{-5} tetrahedron at the similar size of the tetrahedron of SiO_4^{-4}. So it can show similar properties to silica but Al can not form construction units itself.

- It is not a network former but can take place a former role in the silica network. So it is an intermediate.

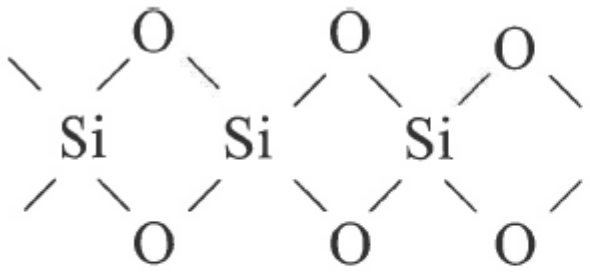

Tetrahedral structure of silica

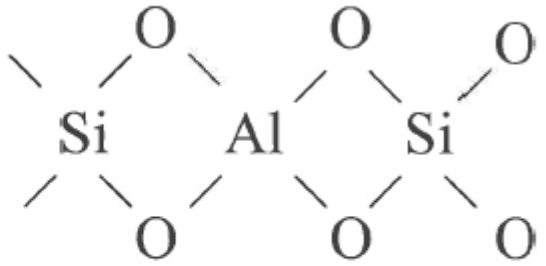

The position of alumina (AlO_4^{-5}) in the silica network

Boron

(network former)

- It stays at the third column (IIIA) of the periodic table like Al.

- It is both a network former like silica and can take place in the silica network as well.

- The coordination number can be three or six fold depending on the network modifiers in the structure whereas silica has a fourfold coordination.

- It has a high attraction force on oxygen in both coordinations resulting a strong B-O bond.

- On the other hand, B-O-B construction units are weaker at higher temperatures. This property brings easier melting and lower viscosity. B keeps this property on both borate glasses (as network former itself) and silicate glasses (as an intermediate).

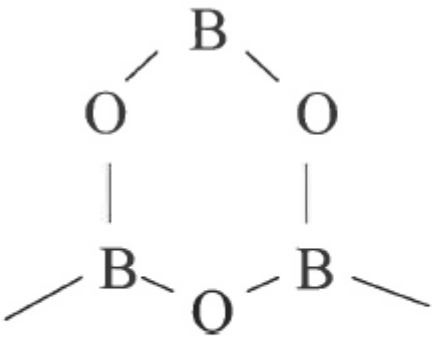

BO_3 network
(trigonal structure)

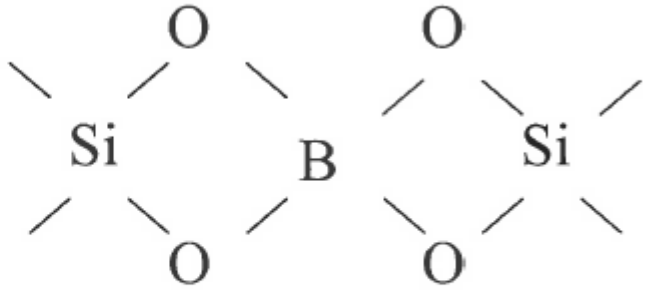

The position of boron in
the silica network

DETERMINATION OF GLASS FORMING ABILITY

Formation of a glass is a rather simple process. The appropriate batch is prepared, placed in a crucible, heated to form a crystal-free melt, and cooled to room temperature. The sample is examined to determine if it contains crystals, using methods ranging from casual visual examination, to X-ray or electron diffraction. If no crystals are detected, the sample is deemed to be a glass; if crystals are detected, it is described as either partially- or fully- crystallized, depending upon the extent of crystallization.

Determination of critical cooling rates can sometimes be carried out using a differential scanning calorimeter (DSC). In this case, the process can be automated, with a computer repeatedly carrying out the experiment with a series of decreasing cooling rates. Cooling rates below the critical will often be characterized by an exothermic peak in the thermal spectrum, due to the release of the heat of crystallization. Absence of such a peak in a thermal spectrum is often taken as evidence of a lack of crystal formation, *i.e.*, glass formation. This technique is best suited for

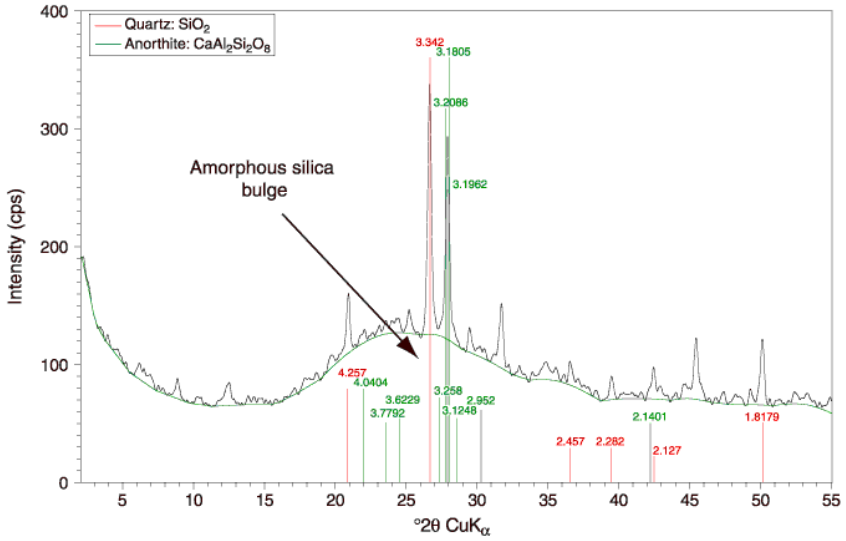

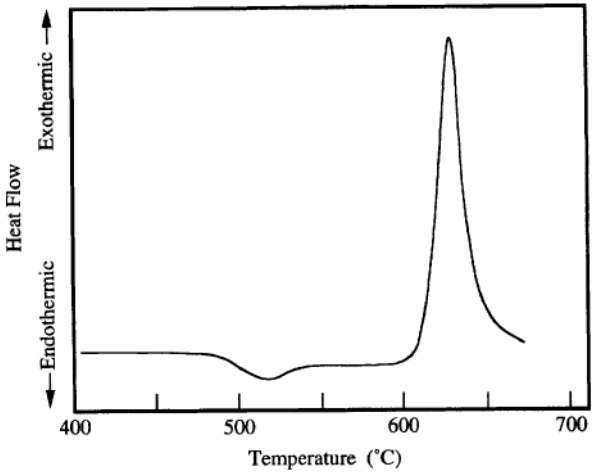

A typical differential scanning calorimeter curve for a glass which forms a single crystalline phase on reheating

Table 3.1 *Raw Materials for Glassmaking*

Common Name	*Nominal Composition*	*Gravimetric Factor**
Albite feldspar	Na_2O–Al_2O_3–$6SiO_2$	Na_2O = 8.46 Al_2O_3 = 5.14 SiO_2 = 1.45
Alumina	Al_2O_3	Al_2O_3 = 1.00
Alumina hydrate	$Al_2O_3 \cdot 3H_2O$	Al_2O_3 = 1.53
Anorthite feldspar	CaO–Al_2O_3–$2SiO_2$	CaO = 4.96 Al_2O_3 = 2.73 SiO_2 = 2.32
Aplite	Alkali lime feldspar	Varies with exact composition
Aragonite	$CaCO_3$	CaO = 1.78
Bone ash	$3CaO–P_2O_5$ or $Ca_3(PO_4)_2$	CaO = 1.84 P_2O_5 = 2.19
Barite (barytes) (Heavy spar)	$BaSO_4$	BaO = 1.52
Borax	$Na_2O–2B_2O_3 \cdot 10H_2O$	Na_2O = 6.14 B_2O_3 = 2.74
Anhydrous borax	$Na_2O–2B_2O_3$	Na_2O = 3.25 B_2O_3 = 1.45
Boric acid	$B_2O_3 \cdot 3H_2O$	B_2O_3 = 1.78
Burnt dolomite	CaO–MgO	CaO = 1.72 MgO = 2.39
Caustic potash	KOH	K_2O = 1.19

Caustic soda	NaOH	$Na_2O = 1.29$
Cryolite	$3NaF–AlF_3$	$NaF = 1.67$ $AlF_3 = 2.50$
Cullet	Scrap Glass	Varies with exact composition
Dolomite	$CaCO_3–MgCO_3$	$CaO = 3.29$ $MgO = 4.58$
Fluorspar	CaF_2	$CaF_2 = 1.00$
Gypsum	$CaSO_4 \cdot 2H_2O$	$CaO = 3.07$
Kyanite	$Al_2O_3–SiO_2$	Varies with exact composition
Lime (quick lime) (Burnt lime)	CaO	$CaO = 1.00$
Limestone (calcite)	$CaCO_3$	$CaO = 1.78$
Litharge (yellow lead)	PbO	$PbO = 1.00$

Microcline	K_2O–Al_2O_3–$6SiO_2$	K_2O = 5.91 Al_2O_3 = 5.46 SiO_2 = 1.54
Nepheline	Na_2O–Al_2O_3–$2SiO_2$	Na_2O = 2.84 Al_2O_3 = 1.73 SiO_2 = 1.47
Nepheline syenite	Mixture of nepheline and feldspars	Varies with exact composition
Niter (saltpeter)	KNO_3	K_2O = 2.15
Potash	K_2O or K_2CO_3	K_2O = 1.00 K_2O = 1.47
Red lead	Pb_3O_4	PbO = 1.02
Salt cake	Na_2SO_4	Na_2O = 2.29
Sand (Glassmaker's sand) (Potter's flint)	SiO_2	SiO_2 = 1.00
Slag	Blast furnace waste glass	Varies with exact composition
Slaked lime	$CaO{\cdot}H_2O$ or $Ca(OH)_2$	CaO = 1.32
Soda ash	Na_2CO_3	Na_2O = 1.71
Soda niter (Chile saltpeter)	$NaNO_3$	Na_2O = 2.74
Spodumene	Li_2O–Al_2O_3–$4SiO_2$	Li_2O = 12.46 Al_2O_3 = 3.65 SiO_2 = 1.55
Whiting	$CaCO_3$	CaO = 1.79

*Quantity required to yield one weight unit of the glass component.

COMPOSITIONAL NOMENCLATURE

Historically, oxide glass compositions were expressed in terms of weight percentages of the oxide components, in what is known as *oxide formulations*. A composition for a *soda–lime–silicate* glass might thus be given as 15% soda, 10% lime, and 75% silica. The reader is assumed to know that the percentages are based on weights of each component.

Use of the stoichiometry approach for oxide glasses, however, can be much more confusing. Consider, for example, the general formula $xLi_2O–(100–x)SiO_2$, where glasses can be made with x having any value between 0 and 40. If we use the atom% approach, this series of glasses would be described by the general formula $Li_{2x}Si_{(100-x)}O_{(200-x)}$. Certain specific compositions, *e.g.*, $x = 33.33$, can be expressed as either $33.33Li_2O–66.67SiO_2$ or as $Li_{66.7}Si_{66.7}O_{166.7}$ or, with reduction to simpli-

BATCH CALCULATIONS

Glass composition: $20Na_2O–5Al_2O_3–75SiO_2$
Molecular weights of components (in g mol^{-1}):
$Na_2O = 61.98$ $Al_2O_3 = 101.96$ $SiO_2 = 60.09$
Molecular wt of glass:
$(0.20 \times 61.98) + (0.05 \times 101.96) + (0.75 \times 60.09) = 62.56$ g mol^{-1}
Weight fraction of each component:
$Na_2O = (0.20 \times 61.98) \div 62.56 = 0.198$
$Al_2O_3 = (0.05 \times 101.96) \div 62.56 = 0.0815$
$SiO_2 = (0.75 \times 60.09) \div 62.56 = 0.720$
For 100 grams of glass: $Na_2O = 0.198 \times 100 = 19.8$ g
$Al_2O_3 = 0.0815 \times 100 = 8.15$ g
$SiO_2 = 0.720 \times 100 = 72.0$ g

If we use albite feldspar as the source of alumina, we also obtain some of the soda and silica needed for the batch. Using the gravimetric factors for albite in Table 3.1, we find that we that 41.89 g of albite will yield the required 8.15 g of alumina. This amount of albite also yields 4.95 g of soda and 28.89 g of silica (divide the weight of albite by the gravimetric factor to find the yield for a given amount of albite). After subtracting these quantities from the required amounts of soda and sand, we find that we must add 14.85 g of soda and 43.11 g of sand. If we use Na_2CO_3 as the source of the additional soda, we will require $14.85 \times 1.71 = 25.39$ g of Na_2CO_3.
Final Batch: $Na_2CO_3 = 25.39$ g
Albite = 41.89 g
Sand = 43.11 g

Structures of Glasses

The most commonly used models for glass structures today are based on the original ideas of Zachariasen, and are grouped under the term *random network theory*.

The structural model offered by Zachariasen provides an approach for describing network structures, whether or not they are glasses.

ZACHARIASEN'S RULES FOR GLASS FORMATION IN SIMPLE OXIDES

(1) Each oxygen atom is linked to no more than two cations.
(2) The oxygen coordination number of the network cation is small.
(3) Oxygen polyhedra share only corners and not edges or faces.
(4) At least 3 corners of each oxygen polyhedron must be shared in order to form a 3-dimensional network.

STRUCTURAL MODELS FOR SILICATE GLASSES

Vitreous Silica

The structure of *vitreous silica* is readily described by the network structural rules of Zachariasen (Table 5.1). The silicon–oxygen tetrahedron, with a coordination number of 4, serves as the basic building block for the network, as required by the second of Zachariasen's rules. Since these tetrahedra have a high degree of internal order, the short range order of the glass is preserved. These tetrahedra are linked at all four corners (rules 3 and 4) to form a continuous, 3-dimensional network. Each oxygen atom is shared between two silicon atoms, which occupy the centers of linked tetrahedra. Disorder in this structure is obtained by allowing variability in the Si–O–Si angle connecting adjacent tetrahedra.

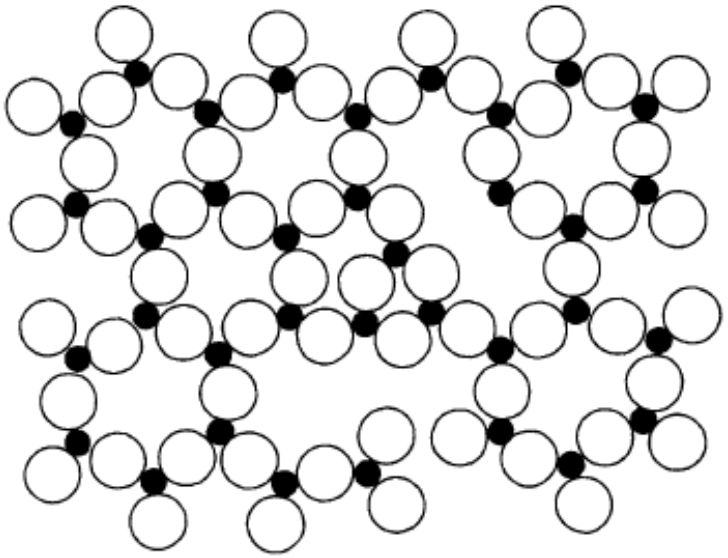

Figure 5.1 *Schematic drawing of a 2-dimensional structure for a pure glassformer. A fourth oxygen would be located above each cation in vitreous silica*

Alkali Silicate Glasses

Alkali silicate glasses, containing large concentrations of alkali oxides, can be easily produced by melting silica with alkali carbonates or nitrates. Glasses containing less than ≈ 10 mol% alkali oxide are considerably more difficult to melt due to their high viscosities.

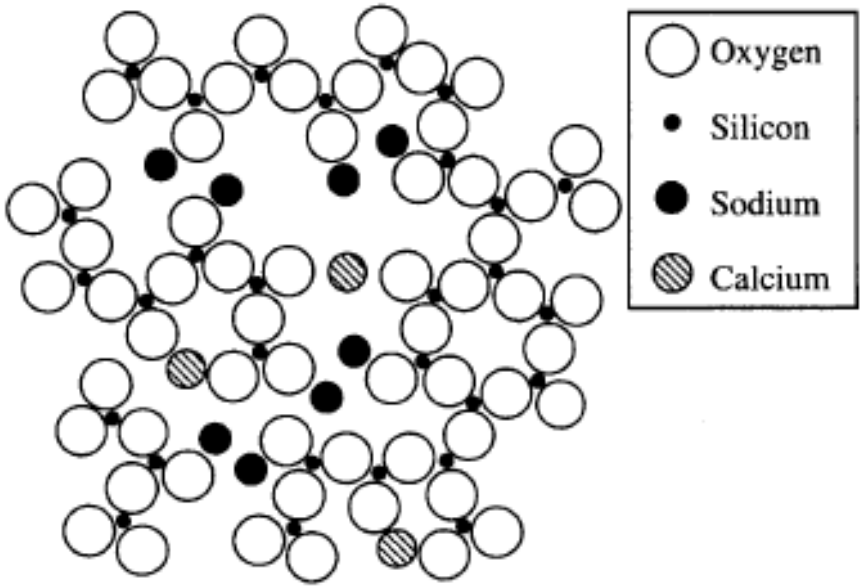

Figure 5.2 *Schematic drawing of a 2-dimensional structure for a soda – lime – silicate glass. A fourth oxygen would be located above each silicon in the 3-dimensional structure*

STRUCTURAL MODELS FOR BORATE GLASSES

Vitreous Boric Oxide

The current model for the structure of vitreous boric oxide differs significantly from that for vitreous silica. Although boron occurs in both triangular and tetrahedral coordination in crystalline compounds, it is believed to occur only in the triangular state in vitreous boric oxide. All such triangles are connected by BO at all three corners to form a completely linked network. However, since the basic building block of this network is planar rather than 3-dimensional, the 3-dimensional linkage which occurs in a network of tetrahedra does not exist for vitreous boric oxide. A 3-dimensional structure is developed by "crumpling" of the network, in much the same way that a two dimensional drawing on a sheet of paper develops a third dimension when the paper is crumpled into a ball. Since the primary bonds exist only within the plane of the paper, bonds in a third dimension (van der Waals bonds in this case) are very weak and the structure is easily disrupted. One result of this structure, for example, can be found in the glass transformation temperature of vitreous boric oxide, which is only $\approx$ 260 °C, as opposed to the T_g of vitreous silica, which is $\approx$ 1100 °C.

Alkali Borate Glasses

Addition of alkali oxides to vitreous silica result in the formation of NBO. Examination of property trends for alkali silicate versus alkali borate glasses, however, suggests that this is not the case for alkali borate glasses. Small additions of alkali oxides to silica cause a decrease in T_g, while similar additions to boric oxide cause an increase in T_g. Conversely, small additions of alkali oxides to silica cause an increase in the thermal expansion coefficient, while similar additions to boric oxide cause a decrease in the thermal expansion coefficient. Any potential structural model for alkali borate glasses must directly address this extreme difference in behavior.

If the effect of alkali oxide additions to boric oxide cannot be explained on the basis of NBO formation, how can they be explained?

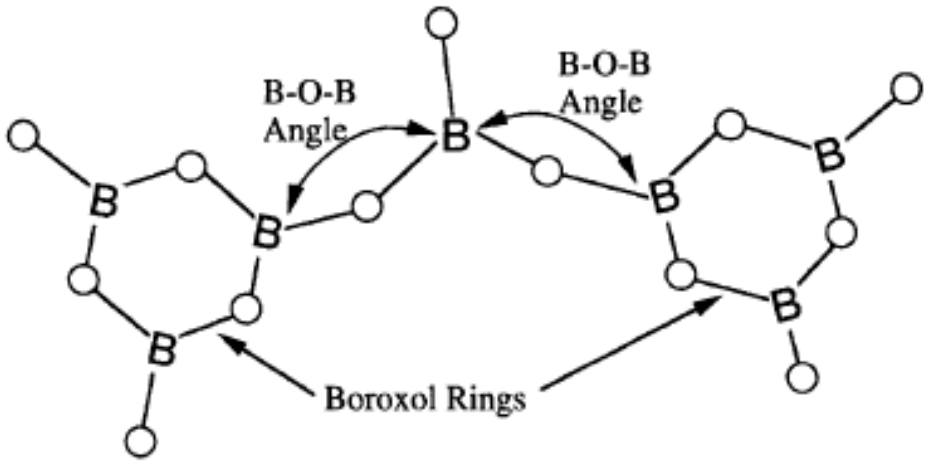

Figure 5.4 *Boroxol ring structures in vitreous boric oxide and alkali borate glasses*

As noted earlier, boron is found in both 3- and 4-fold coordination in oxide crystals. Perhaps the addition of alkali oxide forces some of the boron to change from triangular to tetrahedral coordination, with no NBO formation. Such a change would actually increase the connectivity of the network, increasing T_g and decreasing the thermal expansion coefficient of the glass, which is consistent with experimental observations. Formation of two boron–oxygen tetrahedra would consume the one additional oxygen provided by the R_2O. Since each tetrahedron would be charge deficient by −1 unit, the two alkali oxides would provide sufficient charge compensation for both tetrahedra, in much the same manner as discussed earlier for alkali aluminosilicate glasses. The large $(BO_{4/2})^-$ units now act as anions with a loosely associated alkali cation. A continued increase in the alkali oxide concentration would result in further shift of borons from 3- to 4-fold coordination.

Since such behavior was not observed for the alkali silicate glasses which had been the subject of earlier studies, this behavior was considered to be anomalous for glasses, and hence termed the *borate anomaly*.

Viscosity of Glass Forming Melts

1 INTRODUCTION

The kinetic model of glass formation indicates that the temperature dependence of the viscosity plays a major role in determining the ease of glass formation for any melt. Glasses are most easily formed if either (a) the viscosity is very high at the melting temperature of the crystalline phase which would form from the melt, or (b) if the viscosity increases very rapidly with decreasing temperature. In either case, crystallization is impeded by the kinetic barrier to atomic rearrangement which results from a high viscosity.

In addition to controlling the ease of glass formation, viscosity is also very important in determining the melting conditions necessary to form a bubble-free, homogeneous melt, the temperature of annealing to remove internal stresses, and the temperature range used to form commercial products. The viscosity also determines the upper use temperature of any glass object and the conditions under which *devitrification* (crystallization) may occur. The very high viscosity encountered in the glass transformation range leads to *viscoelastic* behavior, and to time dependence in many of the properties of the melt.

VISCOSITY DEFINITIONS AND TERMINOLOGY

Viscosity is a measure of the resistance of a liquid to shear deformation, *i.e.*, a measure of the ratio between the applied shearing force and the rate of flow of the liquid. If a tangential force difference, F, is applied to two parallel planes of area, A, which are separated by a distance, d, the viscosity, η, is given by the expression:

$$\eta = \frac{Fd}{Av} \tag{6.1}$$

where v is the relative velocity of the two planes.

viscosity is given in N s m^{-2}, or, since a Pascal is a N m^{-2}, is reported in Pa s. Since 1 Pa s = 10 P The viscosity of water at room temperature is $\approx$ 0.01 P, or 0.001 Pa s.

A number of specific viscosities have been designated as reference points on the viscosity/temperature curve for melts. These particular viscosities have been chosen because of their importance in various aspects of commercial or laboratory processing of glass forming melts. Several other reference temperatures which occur at approximate viscosities are also routinely used by glass technologists. These reference points are summarized in Table 6.1, and are shown on a typical curve of viscosity versus temperature for a soda–lime–silica melt in Figure 6.1.

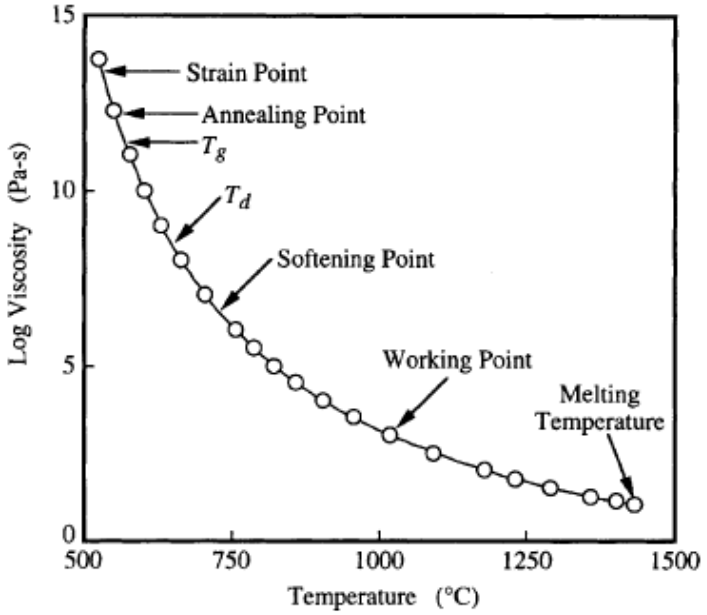

Figure 6.1 *Typical curve for viscosity as a function of temperature for a soda–lime–silica melt (NIST Standard No. 710). Defined viscosity points are indicated on the figure*

Table 6.1 *Viscosity Reference Temperatures*

Name of Reference Temperature	*Viscosity (Pa s)*
Practical Melting Temperature	≈1 to 10
Working Point	10^3
Littleton Softening Point	$10^{6.6}$
Dilatometric Softening Temperature	10^8 to 10^9
Glass Transformation Temperature	$\approx 10^{11.3}$
Annealing Point	10^{12} or $10^{12.4}$
Strain Point	$10^{13.5}$

Fluidity is the reciprocal of the viscosity. A melt with a large fluidity will flow readily, whereas a melt with a large viscosity has a large resistance to flow. While fluidity is often used in dealing with ordinary liquids, virtually all literature dealing with glass forming melts discusses flow behavior in terms of the viscosity.

A number of specific viscosities have been designated as reference points on the viscosity/temperature curve for melts. These particular viscosities have been chosen because of their importance in various aspects of commercial or laboratory processing of glass forming melts. Several other reference temperatures which occur at approximate viscosities are also routinely used by glass technologists. These reference points are summarized in Table 6.1, and are shown on a typical curve of viscosity versus temperature for a soda–lime–silica melt in Figure 6.1.

The viscosity of a typical melt under conditions where fining and homogeneity can be obtained in a reasonable time is termed as the *melting temperature*. Melting usually occurs at a viscosity of ≤10 Pa s

Table 6.1 *Viscosity Reference Temperatures*

Name of Reference Temperature	*Viscosity (Pa s)*
Practical Melting Temperature	≈1 to 10
Working Point	10^3
Littleton Softening Point	$10^{6.6}$
Dilatometric Softening Temperature	10^8 to 10^9
Glass Transformation Temperature	$\approx 10^{11.3}$
Annealing Point	10^{12} or $10^{12.4}$
Strain Point	$10^{13.5}$

Formation of a glass object from a melt requires shaping a viscous mass of liquid, termed a *gob*, by some process involving deformation of the material. The melt must be fluid enough to allow flow under reasonable stresses, but viscous enough to retain its shape after forming. Commercial forming methods require very precise control of the viscosity throughout the forming process, in order to achieve high throughput and high yield of acceptable products. Melt is typically delivered to a processing device at a viscosity of 10^3 Pa s, which is known as the *working point*. Once formed, an object must be supported until the viscosity reaches a value sufficiently high to prevent deformation under its own weight, which ceases at a viscosity of $10^{6.6}$ Pa s, which is termed the *softening point*. The temperature range between the working and softening points is known as the *working range*. Melts which have a large working range are often referred to as *long glasses*, while those with a small working range are called *short glasses*. If the working range occurs at high temperatures relative to the working range of typical soda–lime–silica melts, the composition is termed a *hard glass*. On the other hand, if the working range is below that of soda–lime–silica melts, the composition is termed a *soft glass*. This particular terminology is often confusing since the terms hard and soft in this context do not refer to the resistance to scratching usually designated by these same terms.

The softening point is more properly termed the *Littleton softening point*, after the specific test used to define this reference point. The viscosity of $10^{6.6}$ Pa s does not represent the deformation temperature for all objects. This particular reference point is defined in terms of a well-specified test involving a fiber ≈ 0.7 mm in diameter, with a length of 24 cm. The softening point is defined as the temperature at which this fiber elongates at a rate of 1 mm min^{-1} when the top 10 cm of the fiber is heated at a rate of 5 K min^{-1}. In fact, if the density of the fiber is significantly different from that of a typical soda–lime–silica composition, the viscosity will not be exactly $10^{6.6}$ Pa s at this temperature.

Once an object is formed, the internal stresses which result from cooling are usually reduced by *annealing*. The *annealing point* (cited in various sources as either 10^{12} or $10^{12.4}$ Pa s), which is also determined using a fiber elongation test, is defined as the temperature where the stress is substantially relieved in a few minutes. The *strain point* ($10^{13.5}$ Pa s) is defined as the temperature where stress is substantially relieved in several hours. The strain point is determined by extrapolation of data from annealing point studies. Other tests are also used for these two reference points, with slightly different results.

Two other reference temperatures are often quoted for glass forming melts. While neither of these temperatures represent exact viscosities, they are convenient for relative comparison of the viscosity of different compositions. The *glass transformation temperature*, T_g, can be determined from measurements of the temperature dependence of either the heat capacity or the thermal expansion coefficient during reheating of a glass. This temperature is somewhat dependent upon the property measured, and on the heating rate and sample size used in the measurement. As a result, different studies will report slightly different values for T_g for supposedly identical glasses. Moynihan has shown that the viscosity corresponding to T_g for common glasses has an average value of $10^{11.3}$ Pa s. This value appears to decrease for glasses with very low glass transformation temperatures.

Another viscosity point can be obtained from thermal expansion curves. The *dilatometric softening temperature*, T_d, is usually defined as the temperature where the sample reaches a maximum length in a length versus temperature curve during heating of a glass. This temperature, which will be discussed in more detail in a later chapter, varies slightly with the load applied to the sample by the dilatometer mechanism and the sample size. The viscosity corresponding to T_d lies in the range 10^8 to 10^9 Pa s.

3 VISCOELASTICITY

At low viscosities, glass forming melts usually behave as Newtonian liquids which immediately relax to relieve an applied stress. At extremely high viscosities, however, these liquids respond to the rapid application of a stress as if they were actually elastic materials. It follows that there must exist an intermediate range of viscosities where the response of these melts to application of a stress is intermediate between the behavior of a pure liquid and that of an elastic solid. Since this behavior has aspects of both viscous flow and elastic response, it is known as *viscoelasticity*, or viscoelastic behavior.

Since the response of a liquid to application of an external stress is dependent upon the rate of application of that stress, viscoelasticity can occur over a wide range of viscosities. For common rates of stress application, these viscosities lie in the region of the glass transformation range, particularly in the range from 10^{13} to 10^{8} Pa s. The most common basic model for viscoelasticity, known as the *Maxwell model*, is shown in Figure 6.2. The sample is considered to consist of an elastic

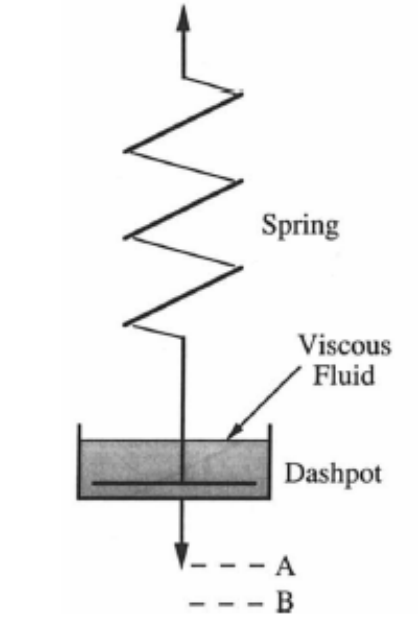

Figure 6.2 *The Maxwell model for relaxation of a viscoelastic material*

5 TEMPERATURE DEPENDENCE OF VISCOSITY

Two mathematical expressions, the Arrhenian equation and the Vogel-Fulcher-Tamman equation, are commonly used to express the temperature dependence of the viscosity of glass forming melts. At one extreme, we find that the viscosity can often be fitted, at least over limited temperature ranges, by an Arrhenian expression of the form:

$$\eta = \eta_o e^{\Delta H\eta/RT} \tag{6.8}$$

where η_o is a constant, ΔH_η is the activation energy for viscous flow, R is the gas constant, and T is the temperature in K. In general, Arrhenian behavior is observed within the glass transformation range (10^{13} to 10^9 Pa s) and at high temperatures where melts are very fluid. The activation energy for viscous flow is much lower for the fluid melt than for the high viscosity of the transformation region. The temperature dependence between these limiting regions is decidedly non-Arrhenian, with a continually varying value of ΔH_η over this intermediate region.

6 COMPOSITIONAL DEPENDENCE OF VISCOSITY

The compositional dependence of the viscosity of glass forming melts is closely related to the connectivity of the structure. In general, changes in composition which reduce connectivity reduce the viscosity, while those which increase connectivity increase the viscosity. These changes are accompanied by changes in fragility which may or may not follow the trend in viscosity, but which are very important in discussion of the temperature dependence of viscosity.

Viscosity data are usually presented in one of two forms. The first form of presentation, which is termed the *isothermal viscosity*, reports the viscosity at specified temperatures. The second form of presentation reports the temperature at which specified viscosities occur, *e.g.*, the values of the Littleton softening temperature or the glass transformation temperature. In general, temperatures referring to a specified viscosity are termed *isokom temperatures* for that viscosity. If a series of curves showing the isokom temperatures are presented on a figure, the individual curves are termed *isokoms* (lines of constant viscosity).

6.1 Silicate Melts

Vitreous silica is the most viscous of all common glass forming melts. The glass transformation temperature of vitreous silica, which is strongly influenced by hydroxyl and other impurity concentrations, lies in the range of 1060 to 1200 °C. The viscosity of silica, which is one of the least fragile melts, varies very slowly with temperature. Production of commercial vitreous silica requires processing temperatures in the range of 2200 °C in order to obtain bubble-free glass.

Addition of alkali oxides to silica results in the formation of non-bridging oxygens and a reduction in the connectivity of the structure. It is not surprising that this reduction in connectivity results in a rapid, monotonic decrease in viscosity with small additions of alkali oxide to silica. The effect of further alkali oxide additions decreases with increasing alkali oxide concentration, and eventually becomes quite small for concentrations exceeding 10 to 20 mol% R_2O. The decrease in viscosity is accompanied by an increase in fragility, which is evidenced by an increase in the reduced activation energy for viscous flow, $\Delta H_\eta/T_g$, in the transformation region and a decrease in ΔH_η in the fluid melt region.

6.2 Borate Melts

The viscosity of vitreous boric oxide is among the lowest reported for common oxide glasses. Boric oxide melts are also considerably more fragile than those of silica, germania, or phosphoric oxide. Since the network of vitreous boric oxide consists of 2-dimensional boron–oxygen triangles, with no strong bonding in 3-dimensions, the connectivity of the network is low. Many of the boron–oxygen triangles are grouped into boroxol rings. Raman spectroscopy has shown that these boroxol rings dissociate with increasing temperature, resulting in a large thermal expansion coefficient for boric oxide melts. It is probable that the fragility of boric oxide melts is a result of the rapid dissociation of the network, which occurs as the boroxol rings open and allow much easier movement within the melt.

Addition of alkali oxides to boric oxide results in considerably more complex behavior than that found for alkali silicate melts. First, even though the connectivity of the melt is increased through conversion of boron–oxygen triangles to tetrahedra with no non-bridging oxygen formation, the fragility of the melt increases with increasing alkali oxide concentration. Second, if we consider the behavior of the viscosity in the transformation region, we find that initial additions of alkali oxide increase the viscosity, while further additions decrease the viscosity, so that maxima in the viscosity versus composition curves occur at 25 to 30 mol% alkali oxide for all 5 alkalis (Figure 6.5). If we examine these curves at high temperatures (> 1000 °C), where the viscosity is $< 10^3$ Pa s, we find that these maxima have disappeared and that the viscosity decreases monotonically with increasing alkali oxide content. Finally,

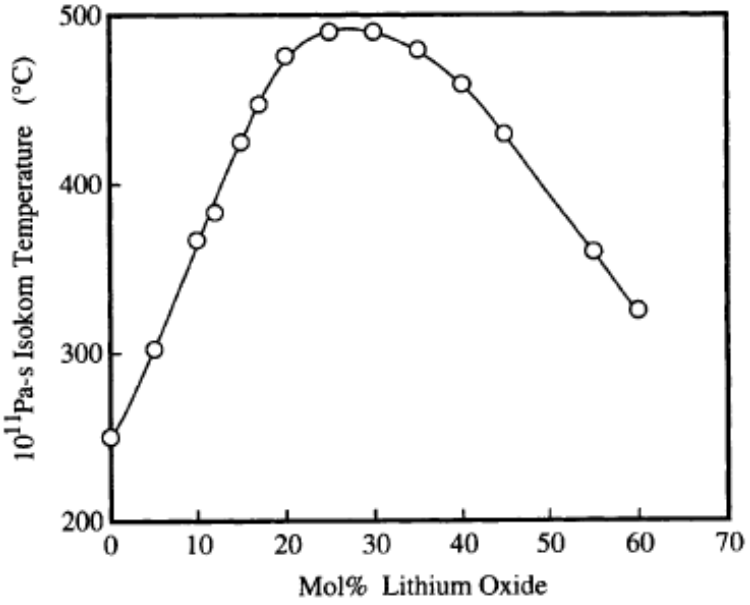

Figure 6.5 *Effect of composition on the 10^{11} Pa s isokom temperature for lithium borate melts*

we also find that the viscosity in the transformation region decreases in the order Li > Na > K > Rb > Cs, which is the reverse of the order observed for alkali silicate melts.

Density and Thermal Expansion

1 INTRODUCTION

Trends in the density, thermal expansion coefficient, refractive index, and viscosity of glasses, as a function of bulk composition serve as the basis for many of the common structural models used today. These models were generated long before Raman, NMR, and other modern spectral techniques were developed. While details of these models have been refined using more sophisticated methods, the basic concepts of network structures, bridging and non-bridging oxygen formation, and changes in coordination number with changes in composition were originally proposed in an attempt to explain trends in property behavior. This approach to glass structure remains common even today, with many structural models proposed on the basis of property studies and later confirmed by the results of spectral studies.

2 TERMINOLOGY

The *density* of a material is defined as the mass of the substance per unit of volume:

$$\rho = \frac{M}{V} \tag{7.1}$$

where ρ is the density, M is the mass, and V is the volume of the sample. If the sample is free of bubbles, voids, or other defects, the calculated density is the *true density* of the material. If, however, the sample contains bubbles, which is occasionally the case for glasses, the calculated density will be less than that of the true density and is termed the *apparent density*. Inclusions with higher densities than the true density, which might, for example, be due to particles of unmelted batch

The *thermal expansion coefficient* of a material is a measure of the rate of change in volume, and therefore density, with temperature. The *true* (sometimes called *instantaneous*) *thermal expansion coefficient* is defined as the slope of the volume *versus* temperature curve, at a specified temperature and constant pressure (usually 1 atmosphere):

$$\alpha_V = \frac{1}{V}\left(\frac{\partial V}{\partial T}\right)_p \tag{7.3}$$

where α_v is the true volume expansion coefficient, V is the volume of the sample, and $(\partial V/\partial T)_p$ is the slope of the curve. The *average*, or mean, *thermal expansion coefficient*, $\bar{\alpha}_v$, which is much more commonly reported, is defined by the change in volume, ΔV, over a specified temperature interval, ΔT:

$$\bar{\alpha}_V = \frac{1}{V}\left(\frac{\Delta V}{\Delta T}\right) \tag{7.4}$$

Although the thermal expansion coefficient is actually defined in terms of the volume of the substance, this value is somewhat difficult to measure. As a result, the expansion coefficient for glasses is usually only determined in one direction, *i.e.*, the measured value is the *linear thermal expansion coefficient*, α_l. The true and average linear thermal expansion coefficients are given by Eqs. 7.3 and 7.4, respectively, where V is replaced by L in each equation. Since glasses are usually isotropic materials with relatively small thermal expansion coefficients, $\alpha_v = 3\alpha_l$ can be used to approximate α_v with very little error in calculation.

Virtually all reported thermal expansion coefficients for glasses are actually average linear thermal expansion coefficients over some specified temperature range. The particular temperature range represented by this value is not always specified in the reported data. Data for commercial glasses are usually obtained for either the range from 0 to 300 °C, 20 to 300 °C, or 25 to 300 °C. Data for experimental studies may be reported for almost any temperature range, so caution must be used when comparing results from different studies. Since the true thermal expansion coefficient can be a strong function of temperature, knowledge of the temperature range used to define an average thermal expansion coefficient is vital for application of the data.

Since most linear thermal expansion coefficients lie between 1 and $50 \times 10^{-6}\ K^{-1}$, metallurgists, ceramists, and other material scientists usually report values with units of ppm K^{-1}. Traditionally, however, glass technologists used $10^{-7}\ K^{-1}$ as the basis for reporting thermal expansion coefficients. A glass technologist might, therefore, indicate that the linear thermal expansion coefficient for a certain glass is 86, while a ceramist might indicate the same coefficient as 8.6. Since older

3 MEASUREMENT TECHNIQUES

3.1 Density

The most direct method for determining density involves weighing a sample of known geometry, calculating its volume from its dimensions, and using Eq. 7.1 to calculate the density. If the available samples do not have simple geometries, we can use Archimedes' principle to determine the volume by liquid displacement. The sample is weighed both in air and suspended in a liquid of known density. The difference in weight equals the weight of the displaced liquid. Since we know the density of the liquid, ρ_L, we can calculate the displaced volume using Eq. 7.1. Dividing the weight of the sample in air, W, by the volume of liquid displaced then yields the density of the sample. The density is calculated from the expression:

$$\rho = \frac{W \rho_L}{(W - W_s)} \tag{7.5}$$

where W_s is the suspended weight of the sample. The choice of the

3.2 Thermal Expansion Coefficients

Almost all reported thermal expansion coefficients for glasses have been obtained using some variation of a push-rod dilatometer. In its simplest form, a push-rod dilatometer consists of a cylinder of a material of known thermal expansion coefficient, which is fixed in place at one end and surrounded by a heating device. A sample is placed inside and against the end of this cylinder. A rod of the same material as the cylinder is placed against the sample. The other end of the rod is connected to some device capable of measuring very small changes in the position of the end of the rod. Heating the region containing the sample results in expansion of the surrounding cylinder, the rod, and the sample. If the sample has a different thermal expansion coefficient from that of the apparatus, the end of the rod will be displaced by an amount determined by the sample length and by the difference in thermal expansion coefficients between the sample and the apparatus material. Determination of the true thermal expansion coefficient of the sample requires correcting the displacement versus temperature data for the expansion of the apparatus.

4 DENSITY AND MOLAR VOLUME

The density of a glass is a strong function of its composition. Density is also dependent to a lesser extent on the measurement temperature and the thermal history of the sample. Changes in morphology can have a small effect on density for phase separated glasses. Crystallization of a glass can significantly alter the density, if the density of the crystalline phase is very different from that of the residual glass.

4.1 Compositional Effects

Densities of the common glass forming oxides are less than those of the corresponding crystalline forms of these compounds. Vitreous silica, for example, has a density of ≈ 2.20 g cm^{-3}. This value can be compared with the densities of α-quartz (the room temperature crystalline form of silica) of 2.65 g cm^{-3}, β-cristobalite (the least dense crystalline form of silica) of 2.27 g cm^{-3}, and coesite (a very dense crystalline form of silica obtained at high pressures) of ≈ 3.0 g cm^{-3}. If we calculate the *free volume*, V_f, of the glass using the simple relationship:

$$V_f = 1 - \frac{V_x}{V_g} \tag{7.6}$$

where V_x is the molar volume of the crystalline form and V_g is the molar volume of the glass, we obtain a value of 0.27, or 27%, for vitreous silica, if we base our calculation on the dense crystal coesite. This large free volume implies that the glass has a very large fraction of interstitial space within the network for accommodation of other ions such as the monovalent alkali ions and the divalent alkaline earth ions.

does not swell as it absorbs the liquid). Indeed, we find that the addition of alkali ions to any of the common glass forming oxides results in an increase in density (Figures 7.1 and 7.2). Even Li_2O, which has only half the molecular weight of silica, increases the density of silicate, borate, or germanate glasses when substituted for the basic glass forming oxide.

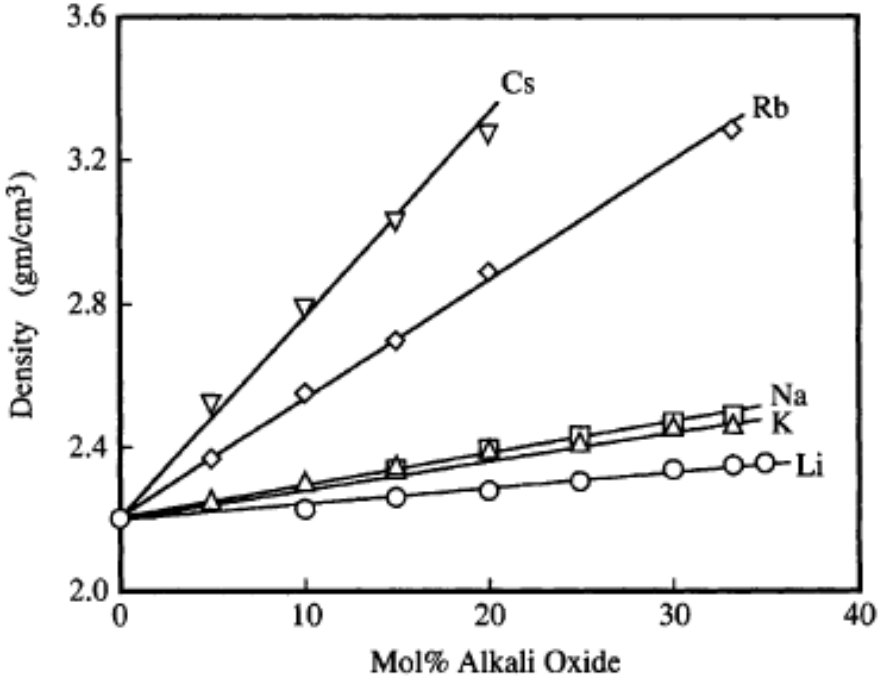

Figure 7.1 *Effect of composition on the density of alkali silicate glasses*

The most dense oxide glasses contain very high concentrations of PbO or Bi_2O_3, with maximum values in the range of 8.0 g cm^{-3} for glasses in the PbO–Bi_2O_3–Ga_2O_3 system. The rather low maximum

Equilibrium Phase Diagrams

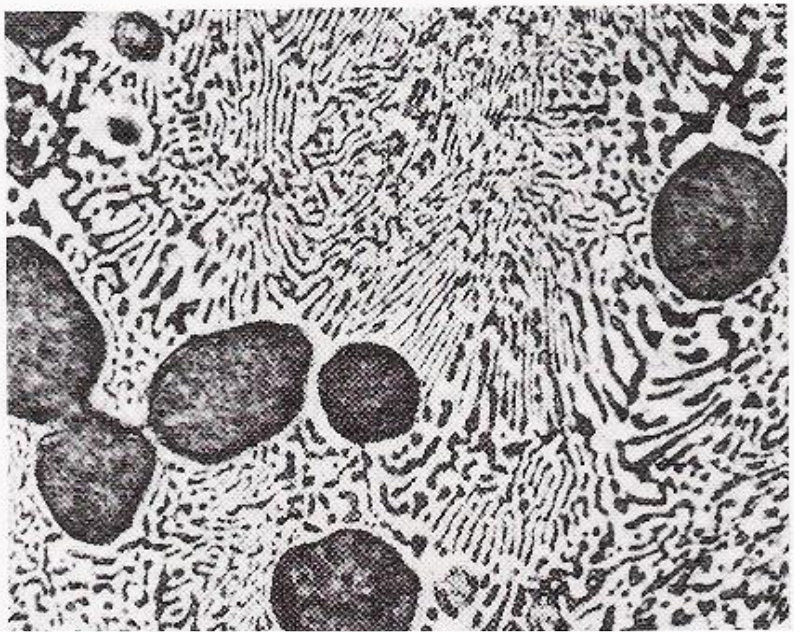

Figure 10.15 Photomicrograph showing the microstructure of a lead–tin alloy of composition 50 wt% Sn–50 wt% Pb. This microstructure is composed of a primary lead-rich α phase (large dark regions) within a lamellar eutectic structure consisting of a tin-rich β phase (light layers) and a lead-rich α phase (dark layers). 400×. (Reproduced with permission from *Metals Handbook*, Vol. 9, 9th edition, *Metallography and Microstructures*, American Society for Metals, Materials Park, OH, 1985.)

A brief introduction of phase diagrams (a more advance course: MME 3008)

Basic definitions

- **System**: specific body of materials under consideration, isolated from the rest of the universe for observation, has a boundary
- **Phase** : any portion of the system (including the whole of the system) that is chemically and physically homogeneous within itself, mechanically separable from the rest of system
- **Components** : smallest number of independently variable chemical constituents, necessary to describe the chemical composition of each phase in the system, e.g. Zn, Au, H_2O, Al_2O_3

Basic definitions

- **Equilibrium**: at *equilibrium* there is a balance between opposing forces acting on the system, system is at its lowest *free energy* state, at *equilibrium* the properties of a system do not change with time, the system is stable
- **Metastable** : reaching *equilibrium* state may take a long time, then the system can exist in a *metastable* state for a very long time.
- **Phase diagram** : a graphic display of phase structure (microstructural) information. Single component phase diagrams are the simplest:

Single-component systems

- H_2O system : water-ice-vapor; phase of water
- Carbon phase diagram

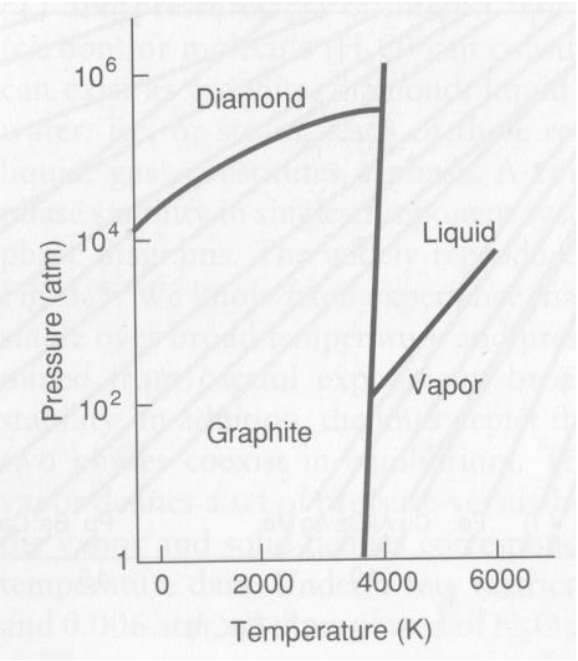

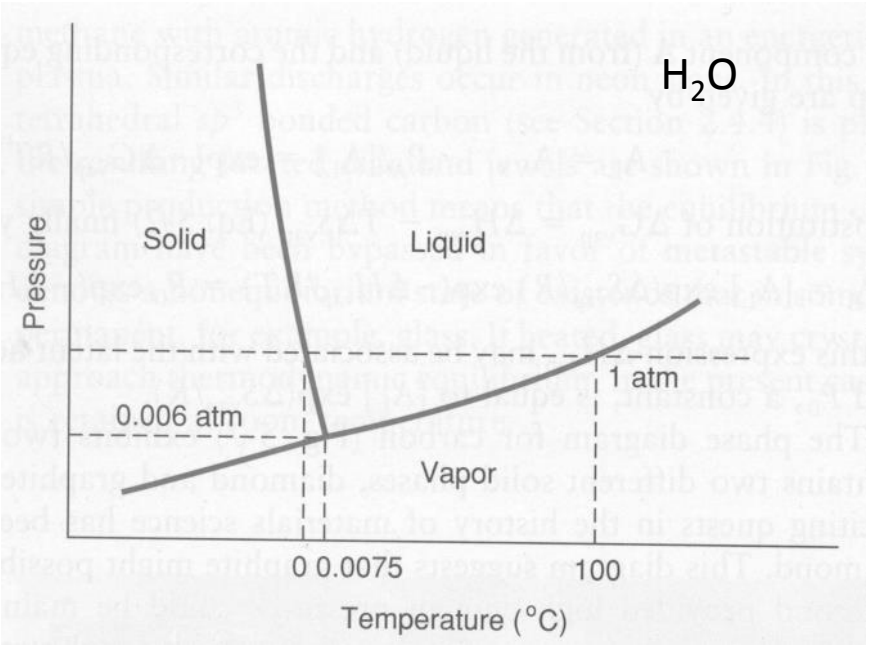

- Temperature and pressure are the independent variables

GIBBS Phase Rule

$$P + F = C + 2$$

- **Degrees of Freedom, F : number of independent variable available to the system**
- **P, number of Phases**
- **C, number of components**
- **Historically, temperature and pressure were the variables available to the system**

GIBBS Phase Rule

- In a single-component system

  F + P = 1 + 2 =>

  We have

  – Di-variant fields

  – Mono-variant lines

  – Invariant point

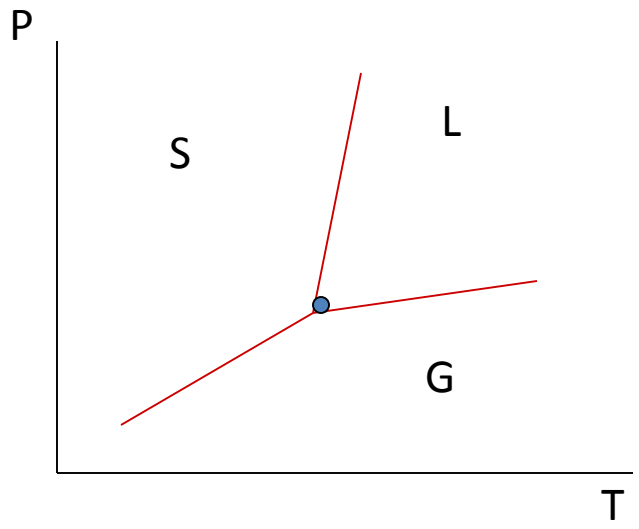

F = number of variables you can change independently without altering the phase composition of the system

Two-components phase diagrams

- Binary phase diagrams with complete solid solubility

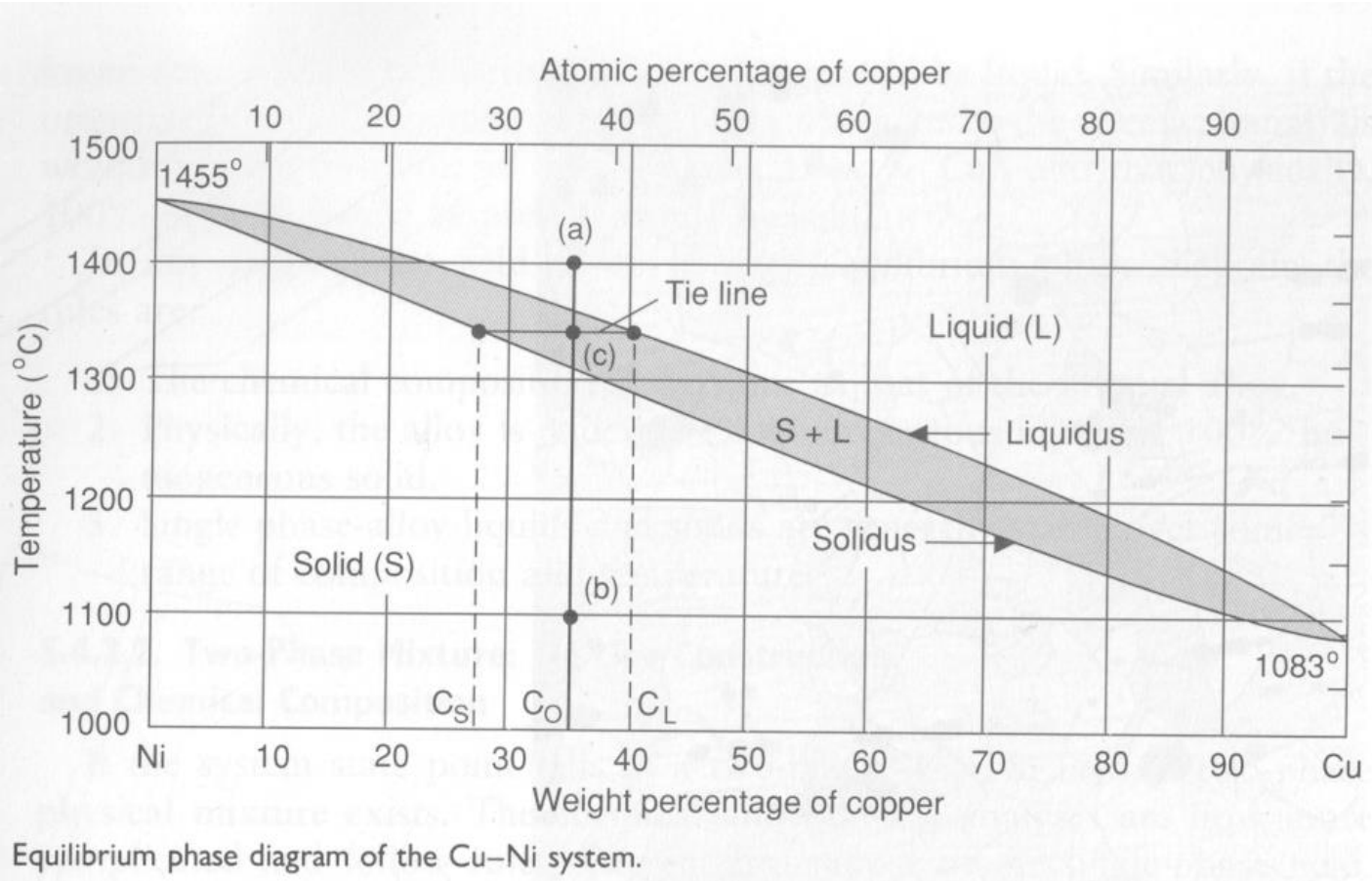

Equilibrium phase diagram of the Cu–Ni system.

- Complete substitutional solid solubility between Cu and Ni
- Cu and Ni both form FCC, have similar atomic radii, similar electro negativity and valences
- Above Liquidus Line @ all T and compositions only liquid present
- Below Solidus Line @ all T and compositions only solid phase present
- Between solidus and liquidus lines two phase region: solid phase and liquid

Finding the compositions of the phases in the two phase region:

Tie-Line construction

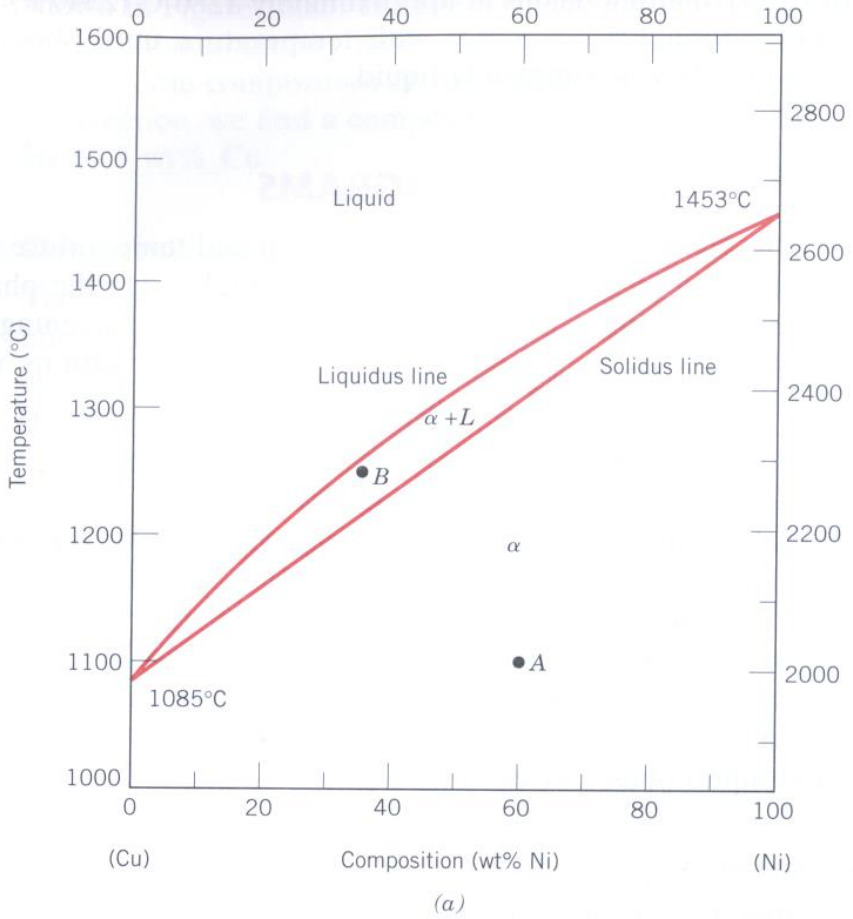

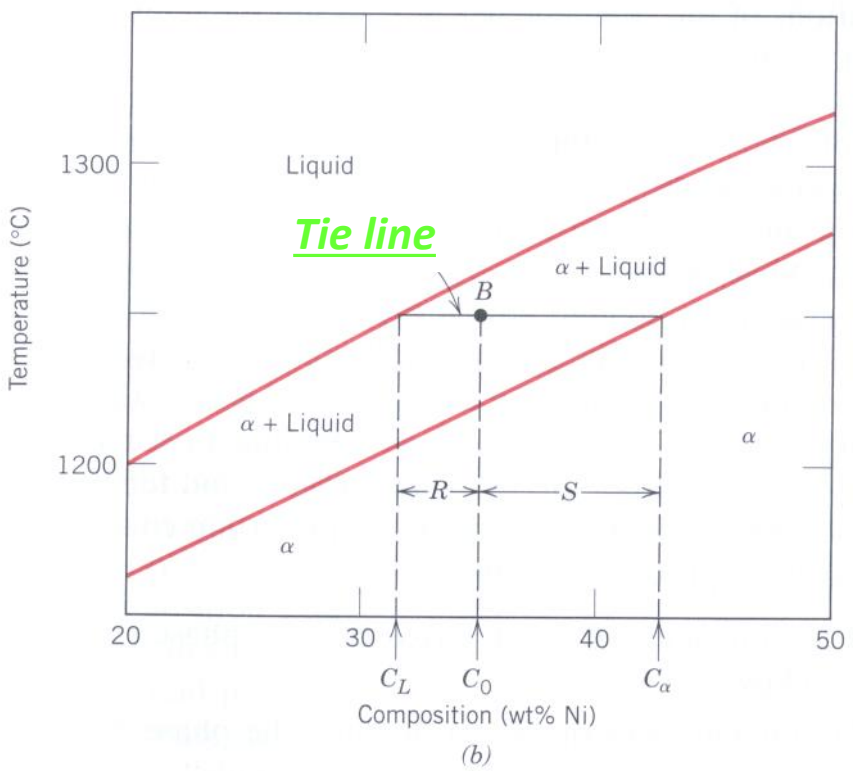

Tie Line construction:

The horizontal line (isotherm) that passes through the two phase regions(and only through two phase regions) and that cuts both the liquidus and the solidus lines is termed a tie line. It connects the two phase compositions.

Composition of the of the liquid is by the intersection point with the liquidus and, similarly, the composition of the solid solution is given by the point of intersection with the solidus.
The relative amounts of the two phases can be calculated easily by the Lever Rule.

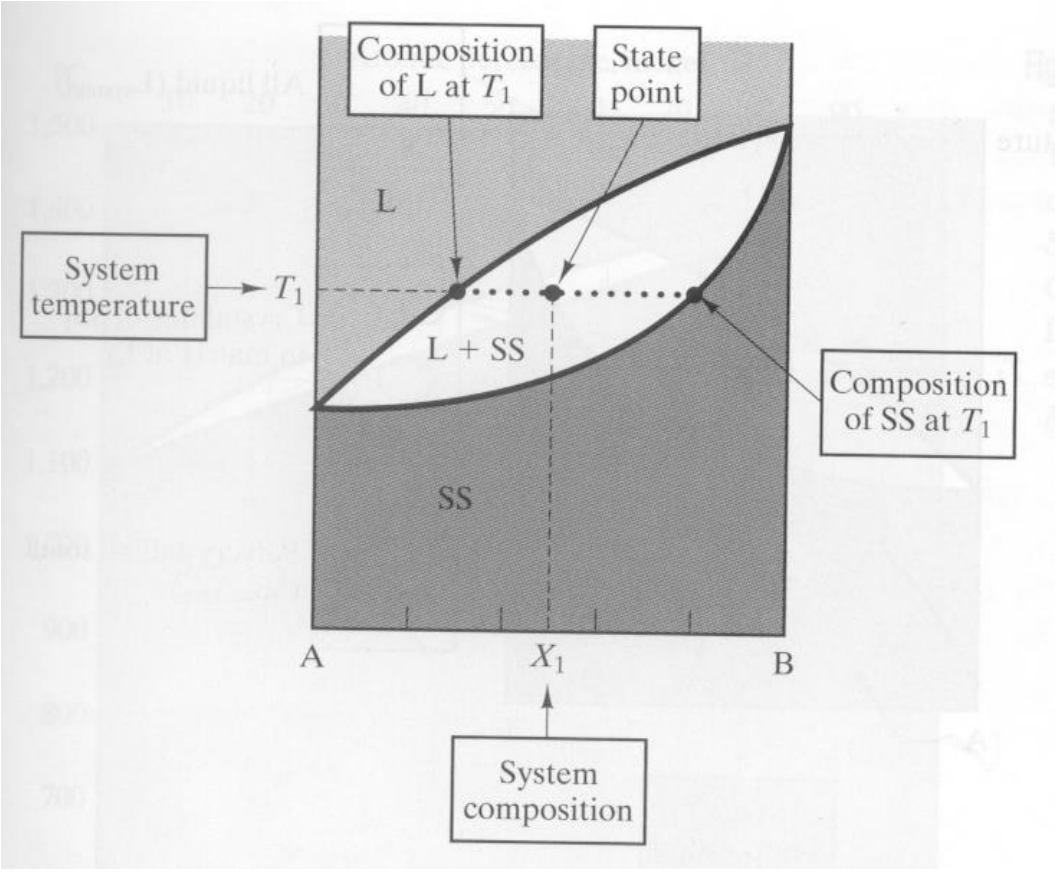

Lever Rule:

Phase diagrams => not only for determining the composition of the phases but also for determining the amounts of phases. The tie line gives the composition of each phase in a two phase region.

The lever rule is based on mass balance.

For two phases a and b;

$$x_\alpha m_\alpha + x_\beta m_\beta = x\,(m_\alpha + m_\beta)$$

Where x_α and x_β are composition of phases and x is overall composition

$$\frac{m_\alpha}{m_\alpha + m_\beta} = \frac{x_\beta - x}{x_\beta - x_\alpha} \quad \text{similarly} \quad \frac{m_\beta}{m_\alpha + m_\beta} = \frac{x - x_\alpha}{x_\beta - x_\alpha}$$

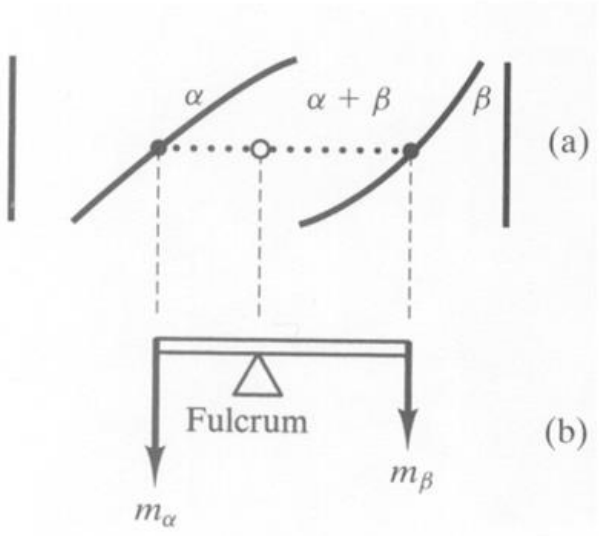

Figure 9.32 *The lever rule is a mechanical analogy to the mass-balance calculation. The (a) tie line in the two-phase region is analogous to (b) a lever balanced on a fulcrum.*

Development of the microstructure: (complete solubility)
Under equilibrium conditions

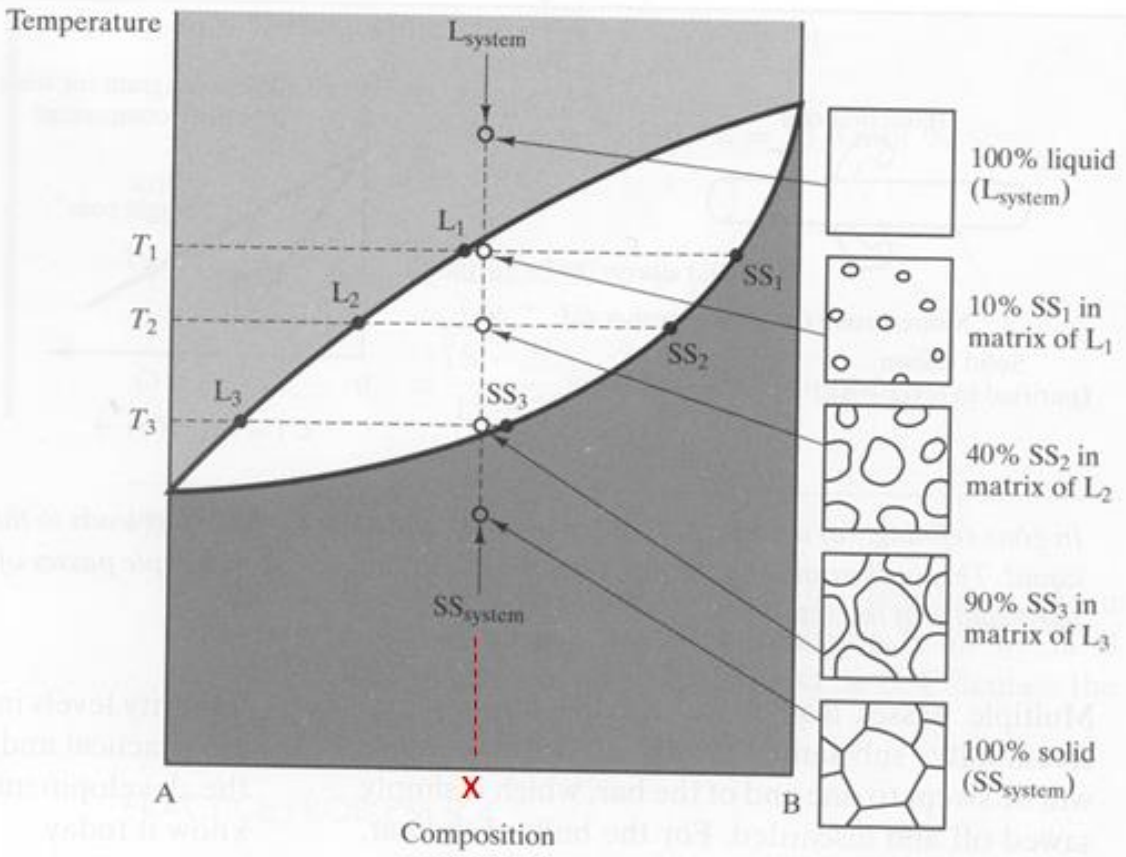

igure 9.33 *Microstructural development during the slow cooling of a 50% A–50% B composition in a phase diagram with complete solid solution. At each temperature, the amounts of the phases in the microstructure correspond to a lever-rule calculation. The microstructure at T_2 corresponds to the calculation in Figure 9.31.*

As a homogeneous liquid with the composition x cools, the contents of a crucible goes through structural changes as one crosses phase boundary lines.

In two phase regions, tie line indicates the compositions of the phases, and the lever rule can be used to find the amounts of phases in the crucible.

At the end of the equilibrium (slow) cooling crucible will contain a homogeneous solid Solution of composition x.

Non-equilibrium cooling Microstructural Development:

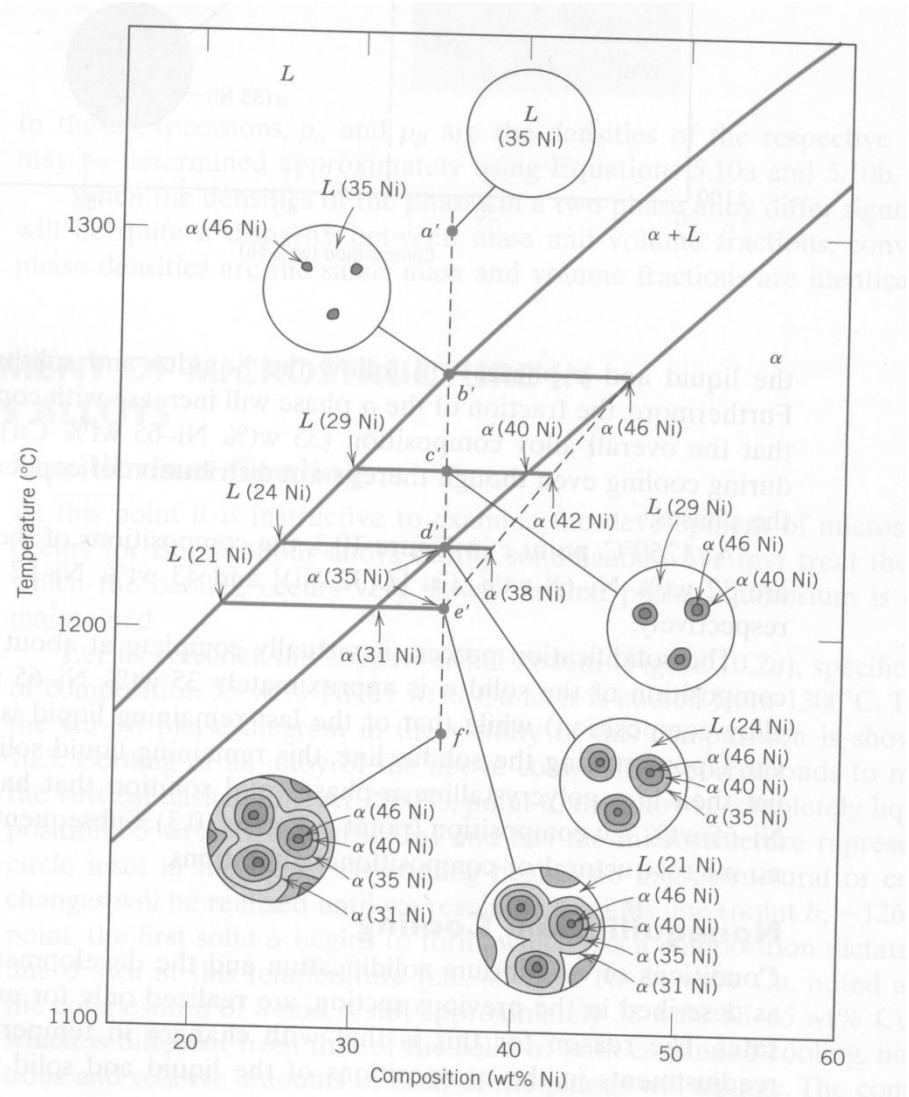

Figure 10.4 Schematic representation of the development of microstructure during the nonequilibrium solidification of a 35 wt% Ni–65 wt% Cu alloy.

Equilibrium solidification requires very slow cooling rates. As T is lowered, liquid and solid have to change compositions according to phase diagram. This requires long range diffusion in liquid and solid. In liquid may be possible since diffusivities are high, but in solid very sluggish diffusion kinetics. =>non-equilibrium microstructure develops (cored). Onion-like microstructure with varying chemical composition; center rich in high melting component, outer layers progressively richer in lower melting compound of the alloy.

Non-equilibrium cooling Microstructural Development:

The average solid and liquid compositions will deviate what the eq. Phase diagram predicts. Deviation is stronger in the phase with the lower diffusion coefficient. Faster cooling rates cause larger deviations from equilibrium. The faster the cooling rate the lower is final solidification Temp.

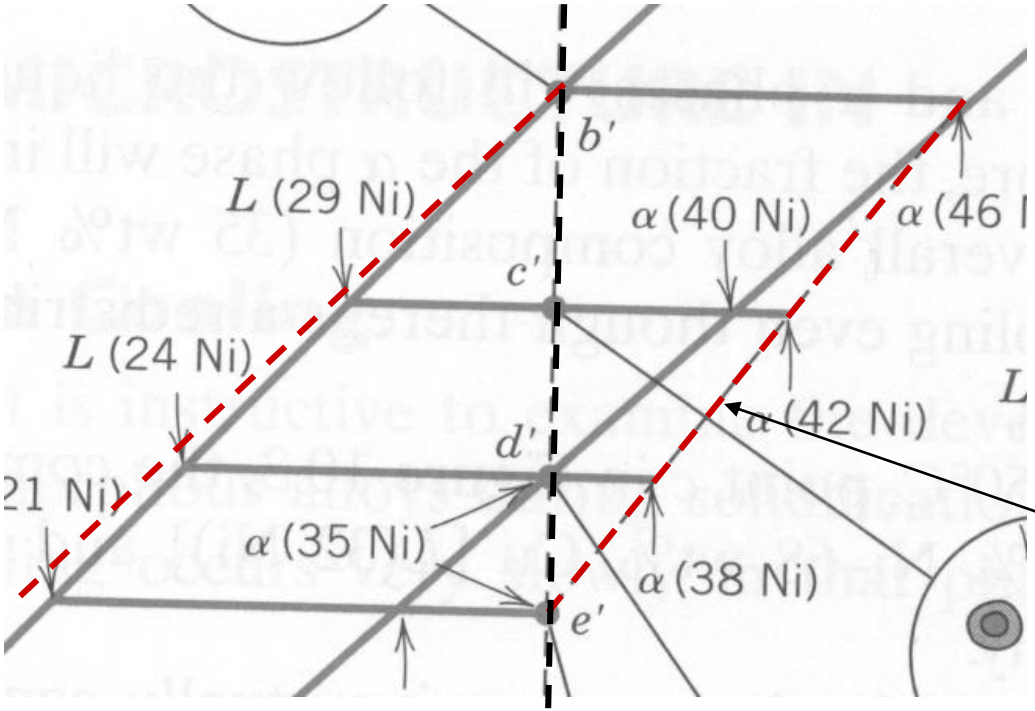

The distribution of the element within the grains will be non uniform. Lower melting component will segregate towards the grain boundaries. This will cause hot-shortness in the "cored" alloy. The grain boundaries in the alloy will melt prematurely as they are richer in the lower melting component.

Average composition of the solid

Binary Eutectic Systems: limited solubility (Under equilibrium conditions)

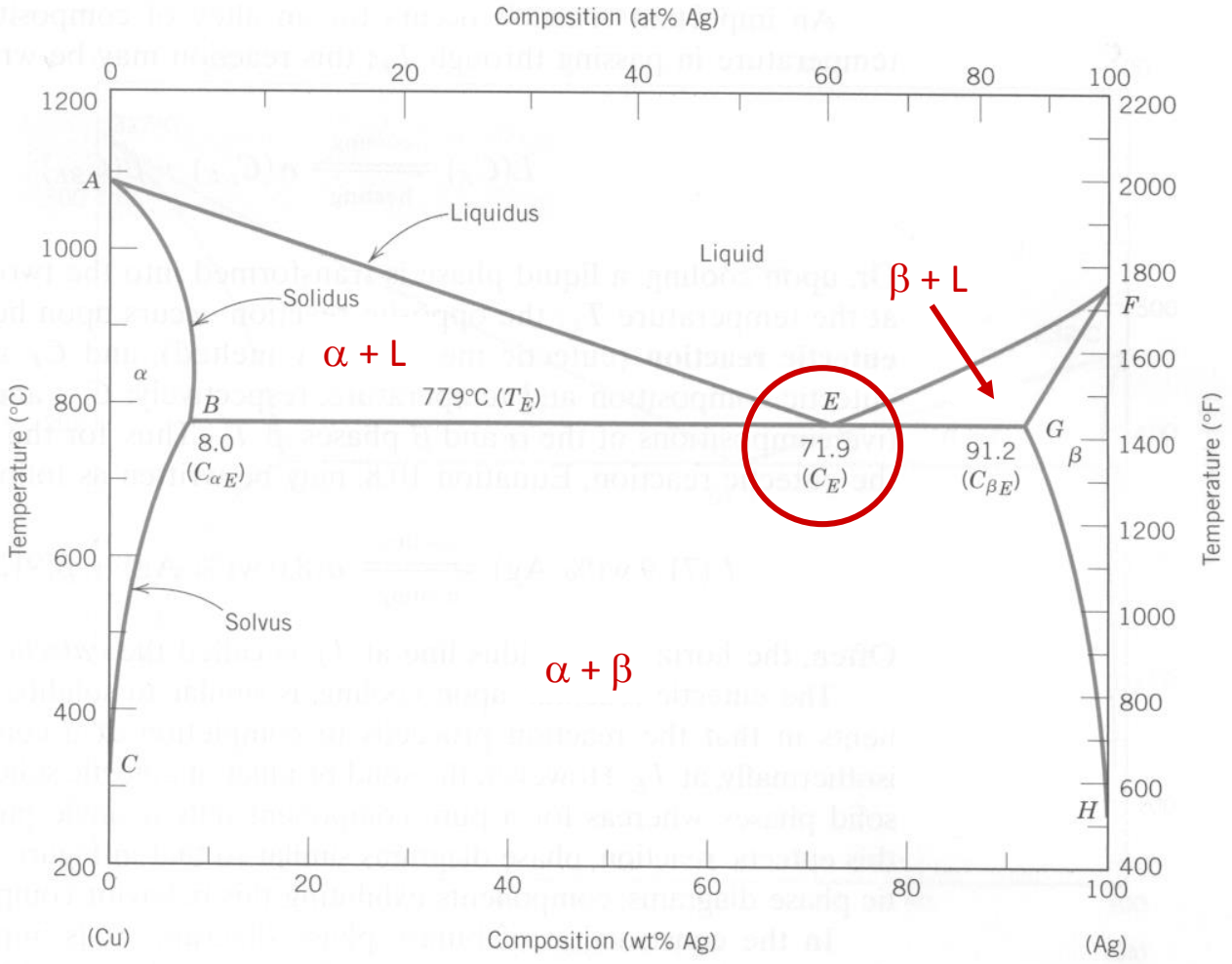

- Three two-phase regions
- Two solid solutions with limited solubility
- A Composition that melts at a lower temperature (Eutectic temp.) than both pure phases, eutectic point, E

Binary Eutectic Systems: limited solubility (Under equilibrium conditions)

@ Eutectic point:

$$L_E \rightarrow \alpha_E + \beta_E \qquad @ \text{ eutectic temperature } T_E$$

- In a eutectic binary phase diagram, three phases can be in equilibrium, at points along the eutectic isotherm.
- Single phase regions are always separated from each other by a two phase region consisting of two single phases that border the two phase region
- The eutectic point, E is the invariant point in the system

Development of the microstructure: Eutectic system

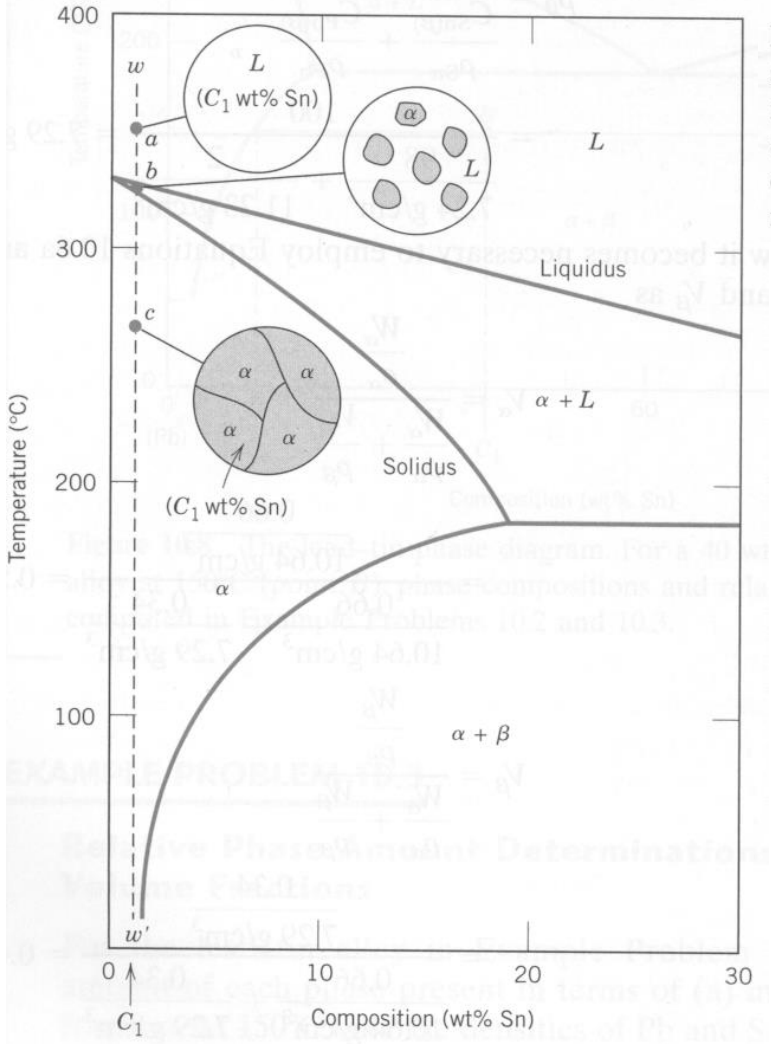

Figure 10.9 Schematic representations of the equilibrium microstructures for a lead–tin alloy of composition C_1 as it is cooled from the liquid-phase region.

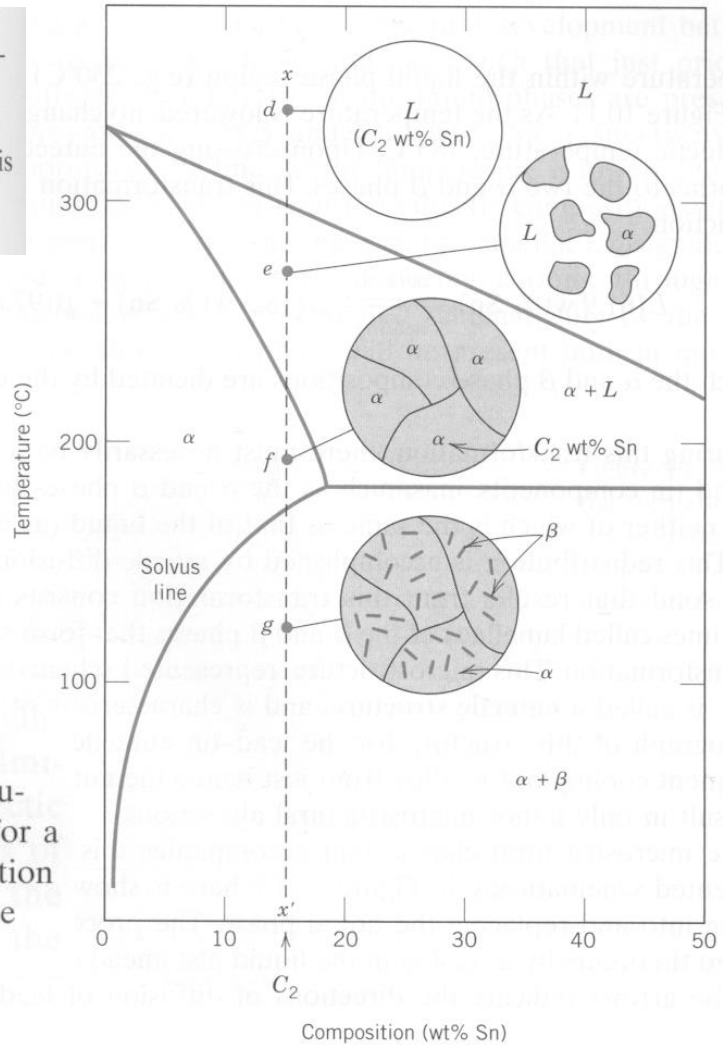

Figure 10.10 Schematic representations of the equilibrium microstructures for a lead–tin alloy of composition C_2 as it is cooled from the liquid-phase region.

Development of the microstructure: Eutectic system

eutectic reaction and eutectic microstructure

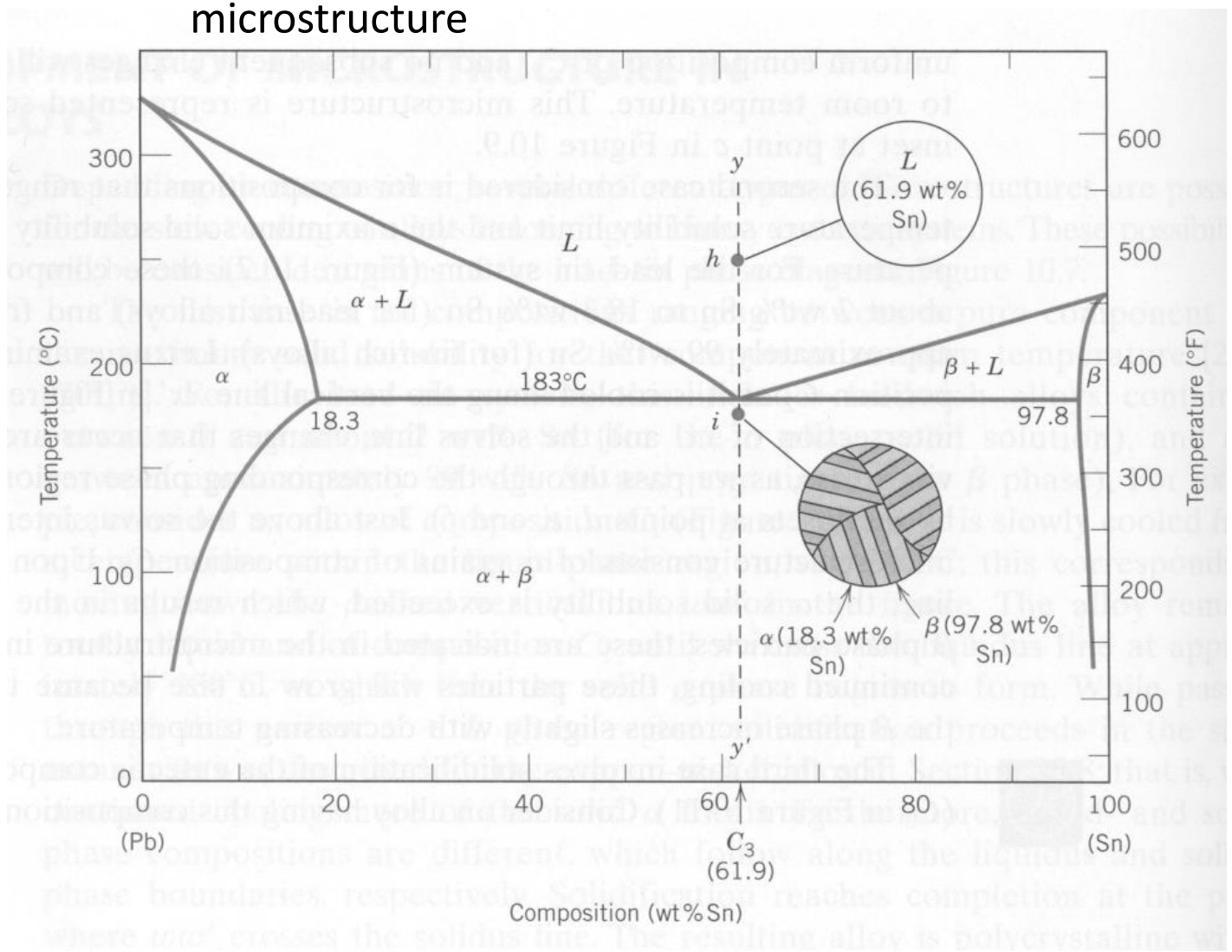

Development of the microstructure: Eutectic system

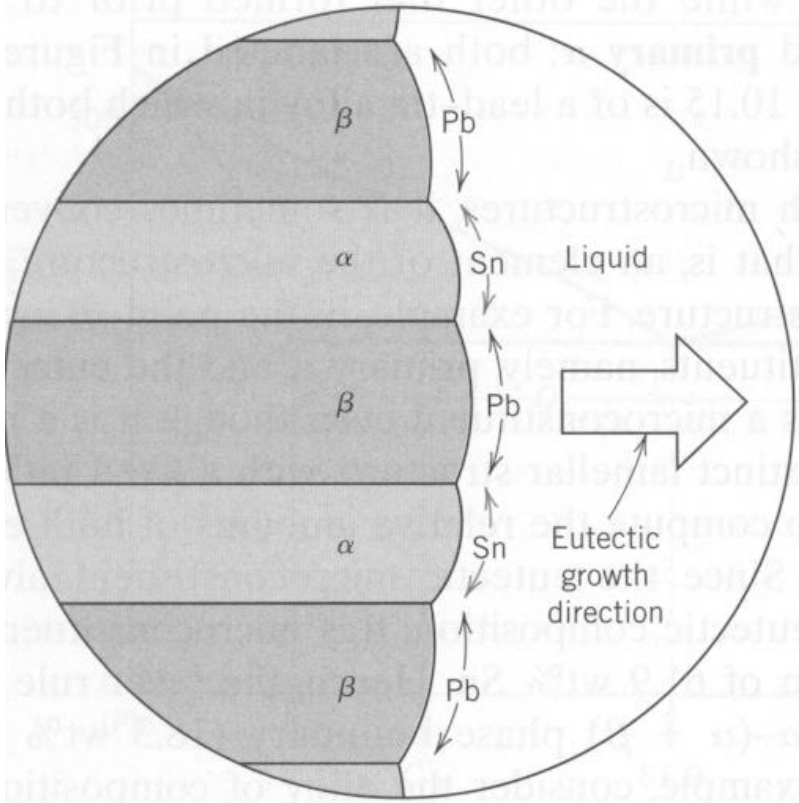

Figure 10.13 Schematic representation of the formation of the eutectic structure for the lead–tin system. Directions of diffusion of tin and lead atoms are indicated by colored and black arrows, respectively.

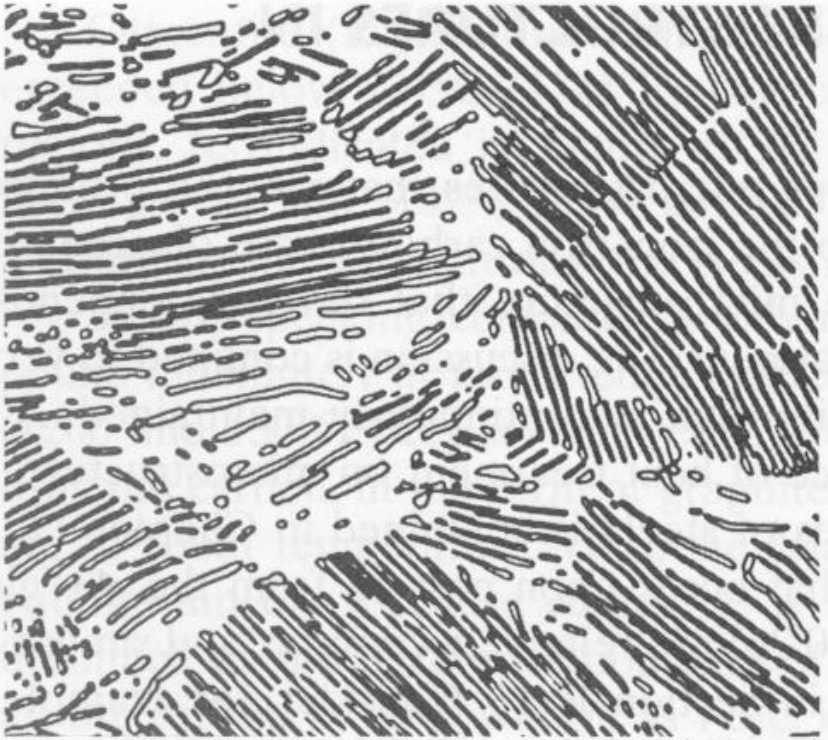

Development of the microstructure: Eutectic system

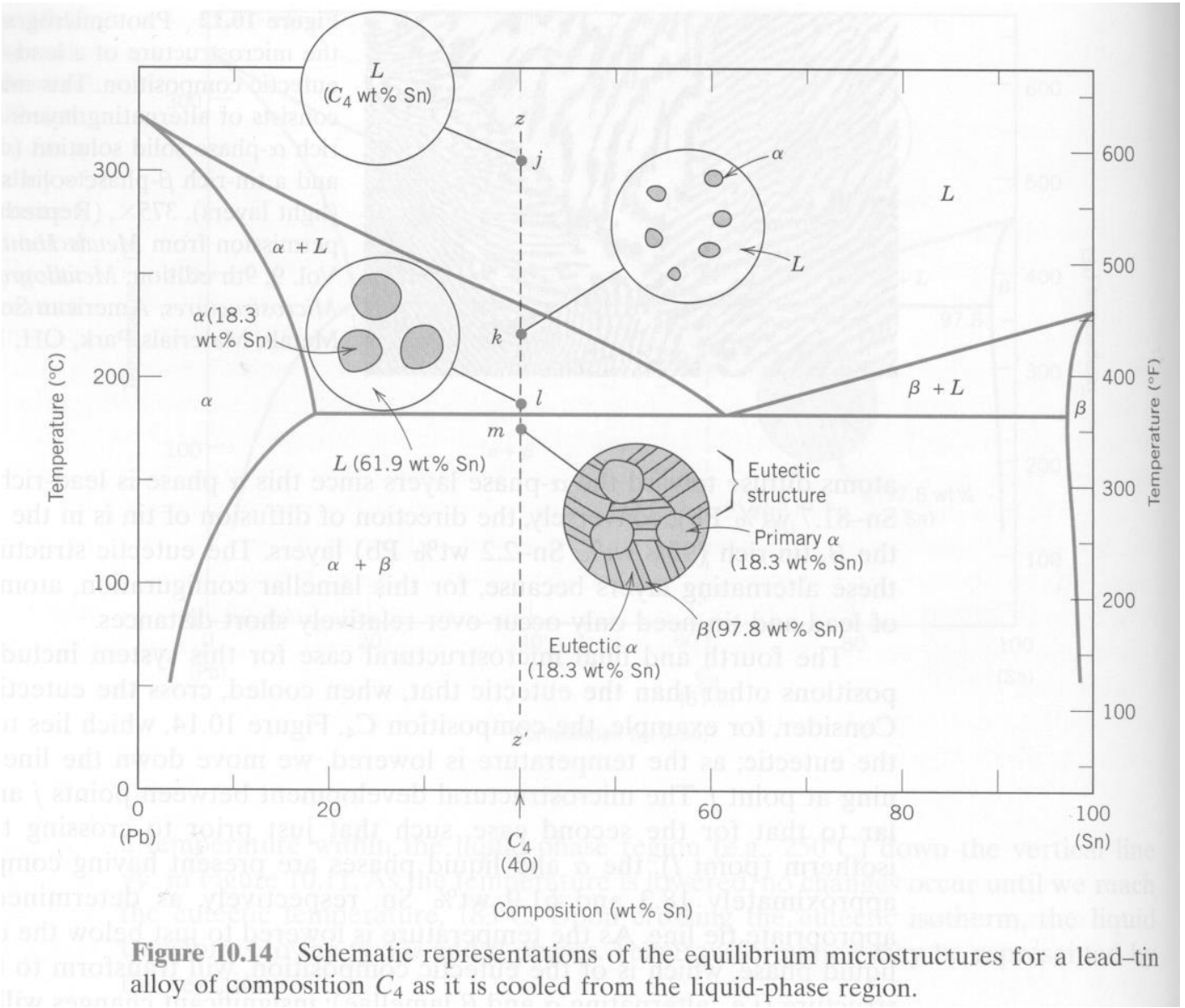

Figure 10.14 Schematic representations of the equilibrium microstructures for a lead–tin alloy of composition C_4 as it is cooled from the liquid-phase region.

Binary phase diagrams with intermediate compounds

Simplest case a congruently melting binary compound

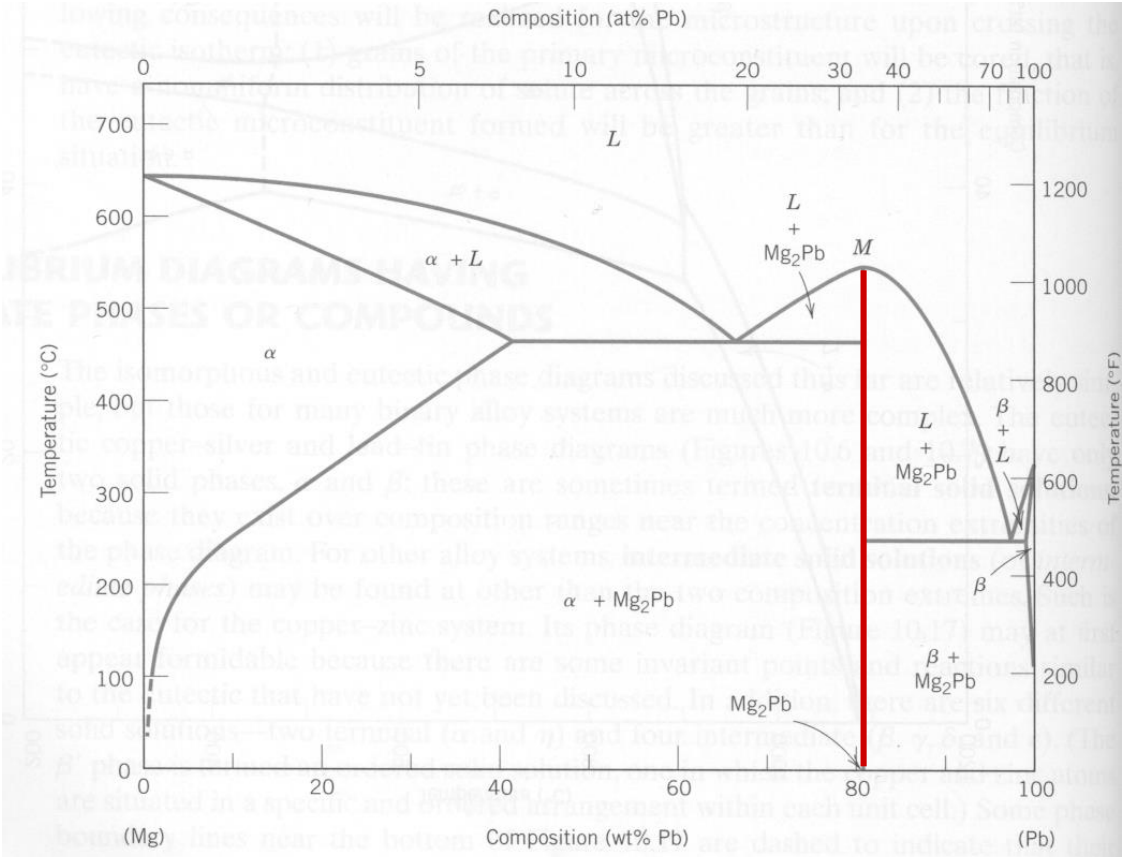

Figure 10.18 The magnesium–lead phase diagram. (Adapted from *Phase Diagrams of Binary Magnesium Alloys*, A. A. Nayeb-Hashemi and J. B. Clark, Editors, 1988. Reprinted by permission of ASM International, Materials Park, OH.)

- A congruently melting compound divides a simple eutectic into two simple eutectics.
- The compounds melts directly into a liquid with the same composition

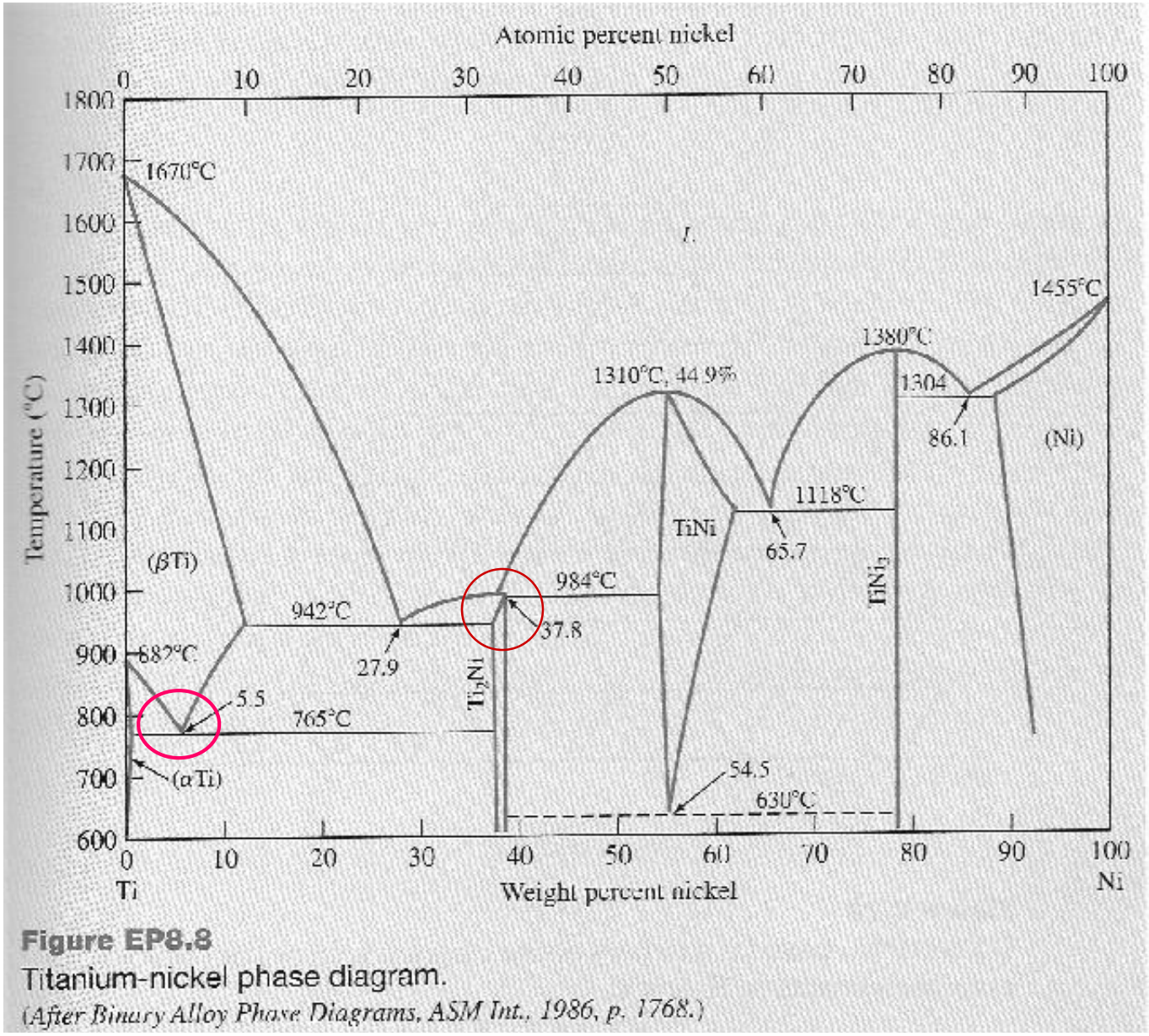

Figure EP8.8
Titanium-nickel phase diagram.
(After Binary Alloy Phase Diagrams, ASM Int., 1986, p. 1768.)

Even this one is not too bad. There are two new types of reactions: Eutectoid and Peritectic reactions; besides there are intermediate compounds that have solubilities on both sides; e.g. TiNi

Eutectoid and Peritectic reactions:

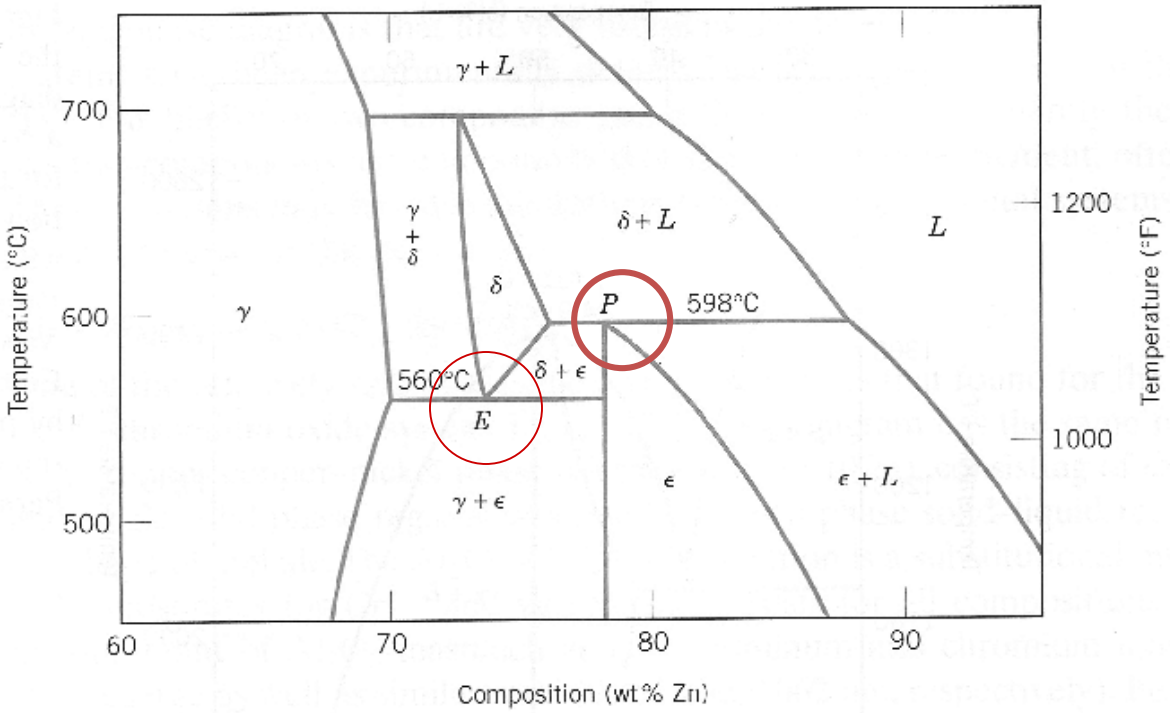

Figure 10.19 A region of the copper–zinc phase diagram that has been enlarged to show eutectoid and peritectic invariant points, labeled *E* (560°C, 74 wt% Zn) and *P* (598°C, 78.6 wt% Zn), respectively. (Adapted from *Binary Alloy Phase Diagrams*, 2nd edition, Vol. 2, T. B. Massalski, Editor-in-Chief, 1990. Reprinted by permission of ASM International, Materials Park, OH.)

Eutectoid rxn

$\delta \leftrightarrow \gamma + \epsilon$

Peritectic rxn

$\delta + L \leftrightarrow \epsilon$

Ternary Phase Diagrams

- Three component systems **A**, **B** and **C**
- requires that we know the three binary systems for the 3 components
  - **AB**, **BC**, **CA**
- Ternary diagrams present a map of the Liquidus surface which is contoured with respect to Temperature.
- Fields indicated on the ternary diagram represent the primary phase fields present on the Liquidus surface.

Ternary Diagrams - First Step

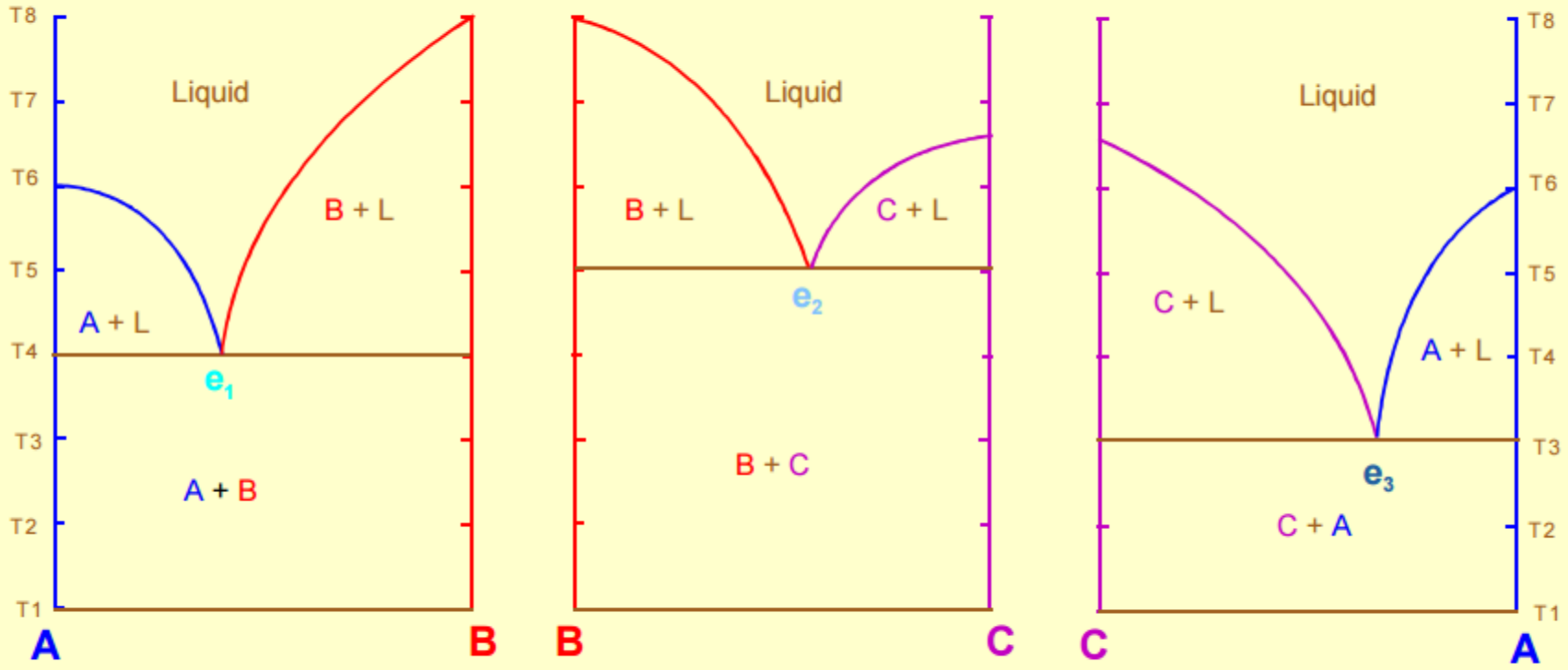

Each Ternary diagram is constructed using the three binary diagrams for the three components **AB**, **BC** and **CA**

Ternary Diagrams - First Step

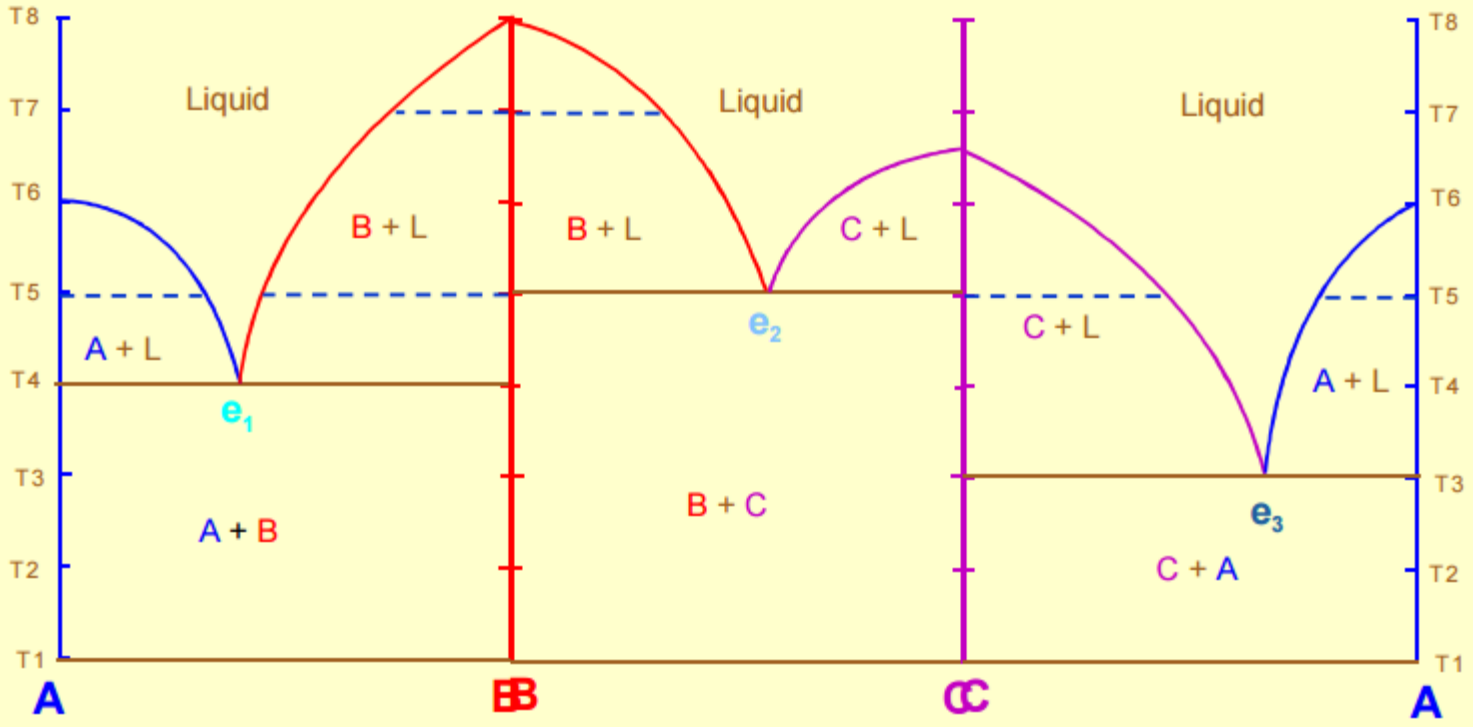

Each Ternary diagram is constructed using the three binary diagrams for the three components **AB**, **BC** and **CA**

Ternary Diagrams - Next Step

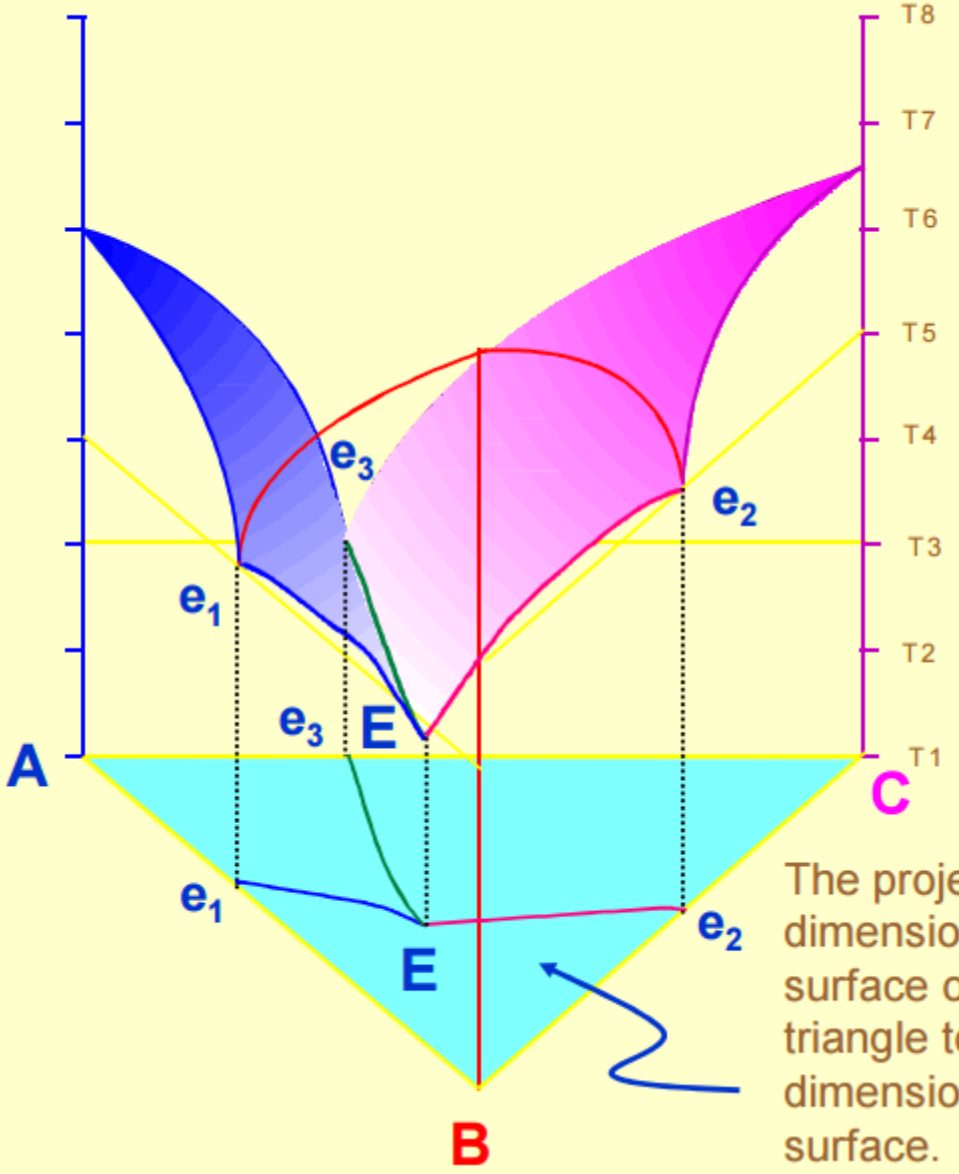

The projection of the three dimensional liquidus surface onto the base of the triangle to present a two-dimensional view of the surface.

Ternary Diagrams

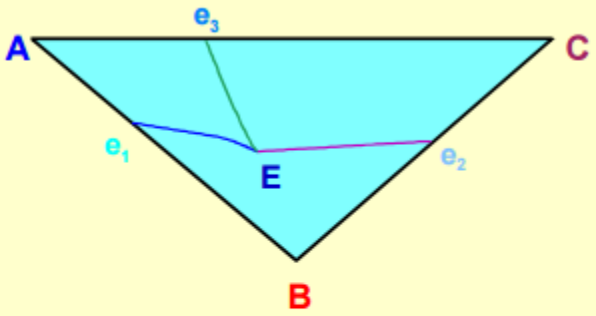

A copy of the base of the triangle onto which the liquidus surface has been projected, showing the location of the binary eutectics (e_1, e_2, e_3) and the ternary eutectic (**E**).

The projected surface above rotated into an upright position and stretched out into an equilateral triangle.

Last Step

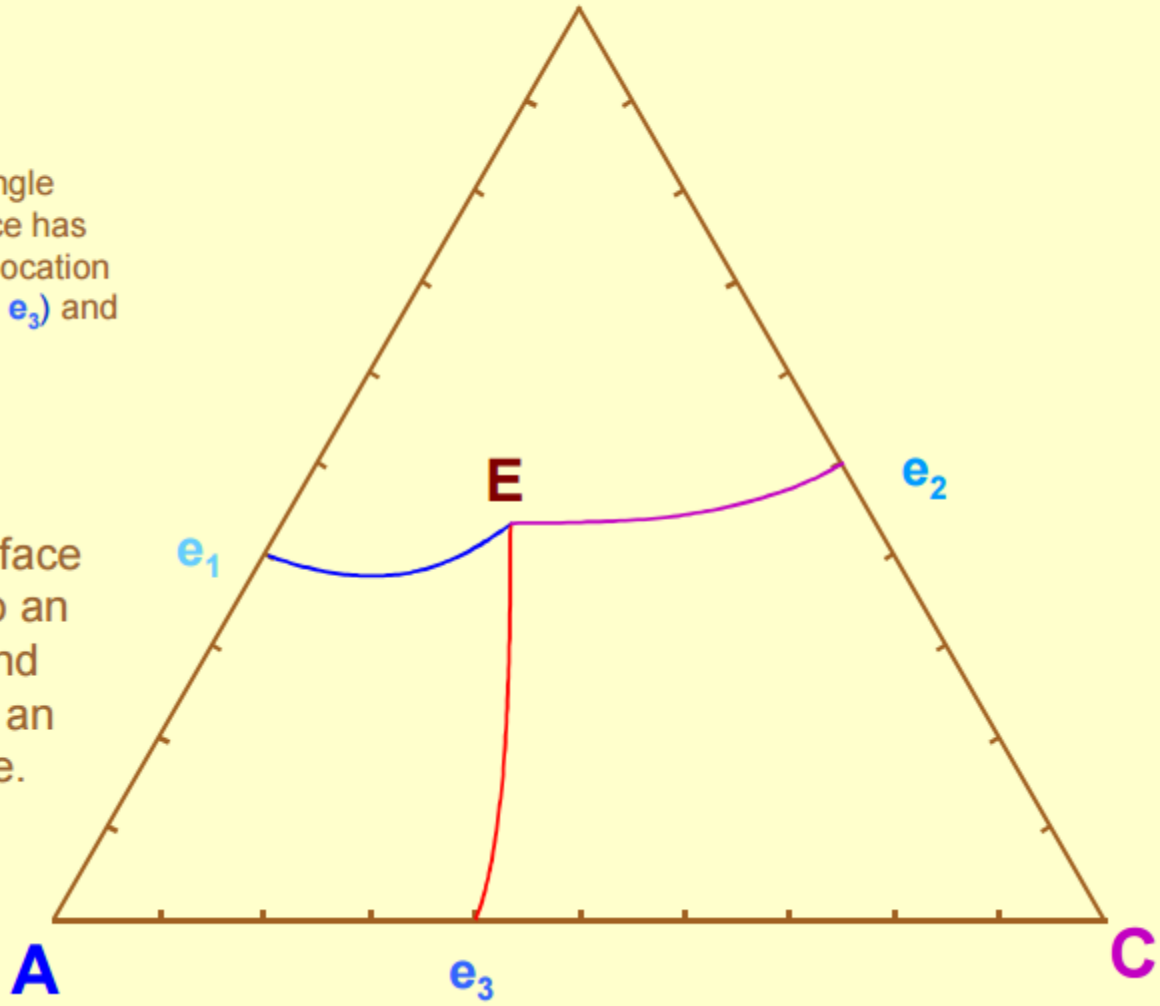

Ternary Diagrams

Phase Rule

$$P + F = C + 1$$

At **Point 1**, which lies in the field **C + L**

P = 2 - **Solid C** and **L**

C = 3 - **A**, **B** and **C**

F = 2

At **Point 2**, which lies on the Boundary Curve separating the fields of **A + L** from **B + L**;

P = 3 - **Solid A**, **Solid B** and L

C = 3 - **A**, **B** and **C**

F = 1

At **E**, all three phase fields meet;

P = 4 - **Solid A**, **Solid B**, **Solid C** and L

C = 3 - **A**, **B** and **C**

F = 0

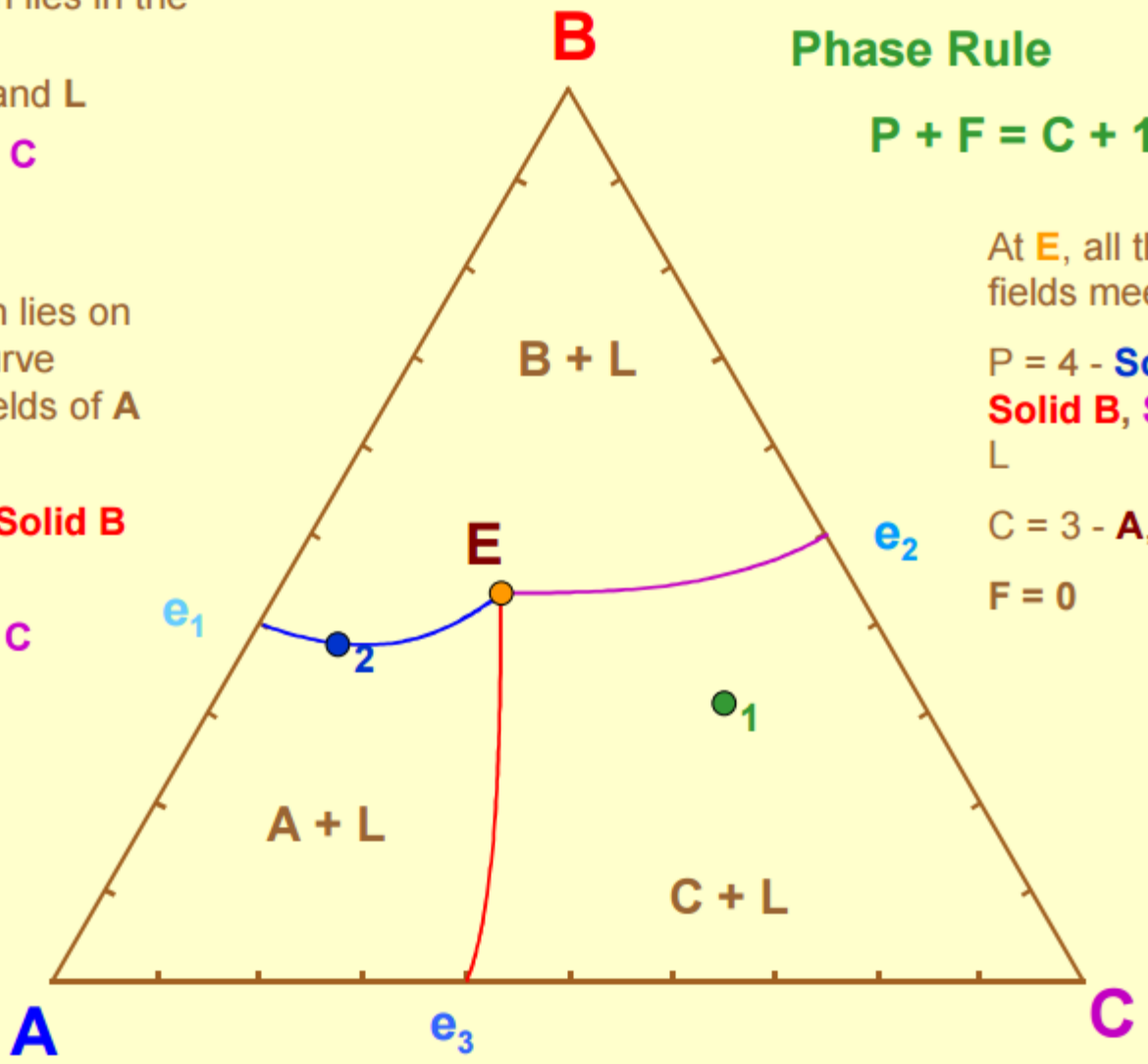

Compositions in Ternary Diagrams

- All compositions e.g. bulk compositions, liquid compositions, solid compositions on ternary diagrams are expressed in terms of the three end-member components which define the system.
- These are located at the apices of the triangle.

Ternary Compositions

The components (**A**, **B** and **C**) which define a ternary diagram are placed at the apices of the triangle.

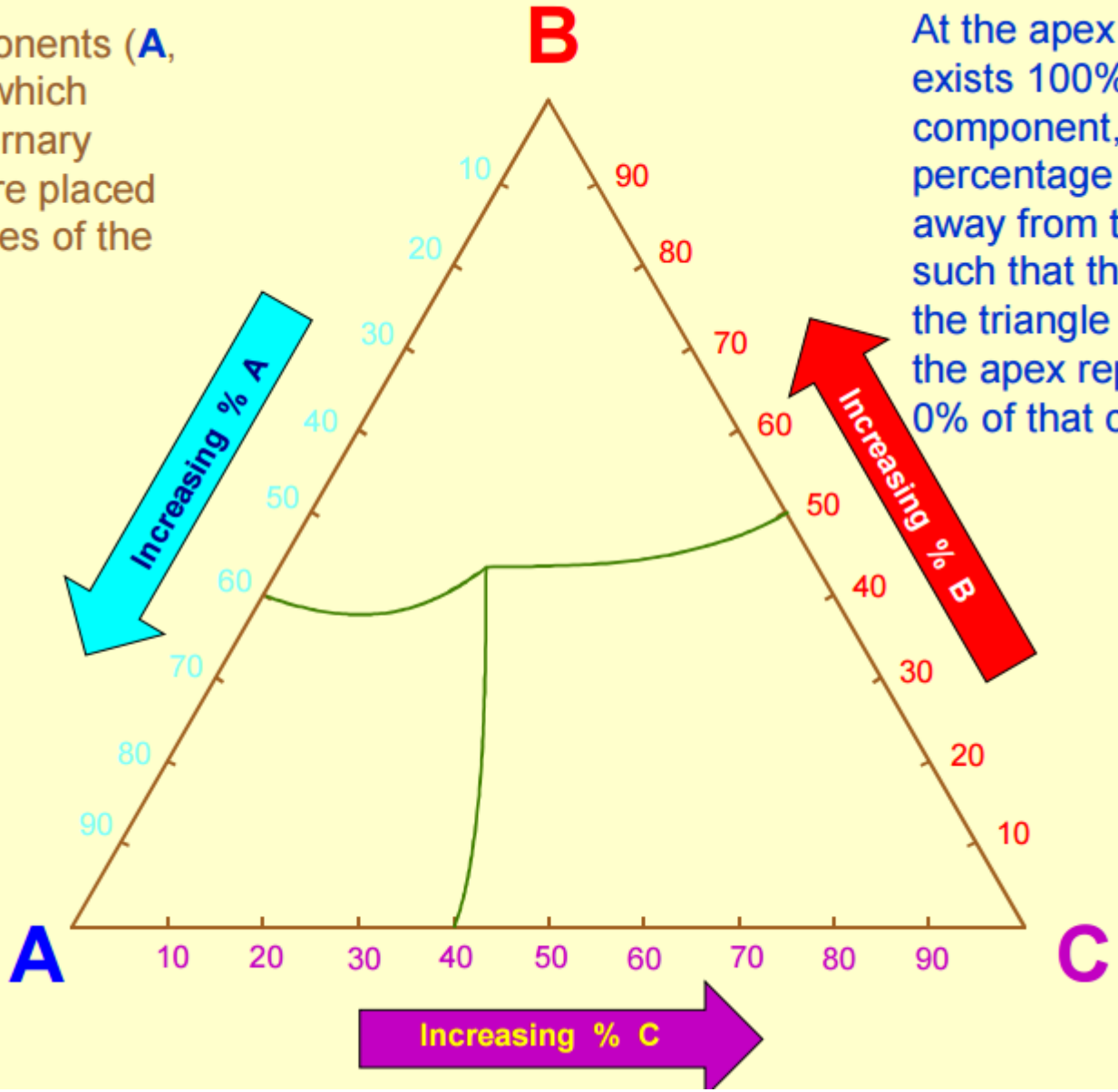

At the apex there exists 100% of that component, with the percentage decreasing away from the apex, such that the side of the triangle opposite the apex represents 0% of that component.

Ternary Compositions

- Compositions of points which lie inside a ternary diagram can be determined by using either of two methods:
  - **Triangular Grid**
  - **Two Line Method**

Triangular Grid Method

- In this method a series of grid lines are constructed.
- The proportion of any point within the triangle can be represented by grid lines drawn through the point of interest, parallel to each side of the triangle.

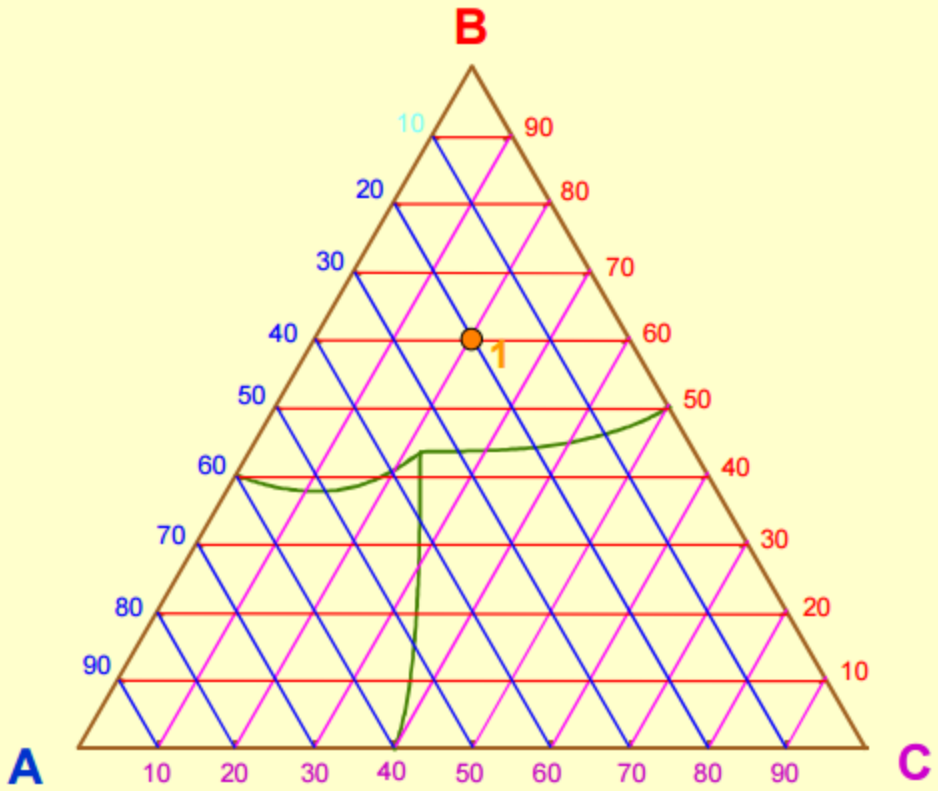

Composition 1

20% A

60% B

20% C

100% Total

Two Line Method

In this method two lines are drawn through the composition point of interest, parallel to any two sides of the triangle.

Composition 1

20% A

60% B

20% C

100% Total

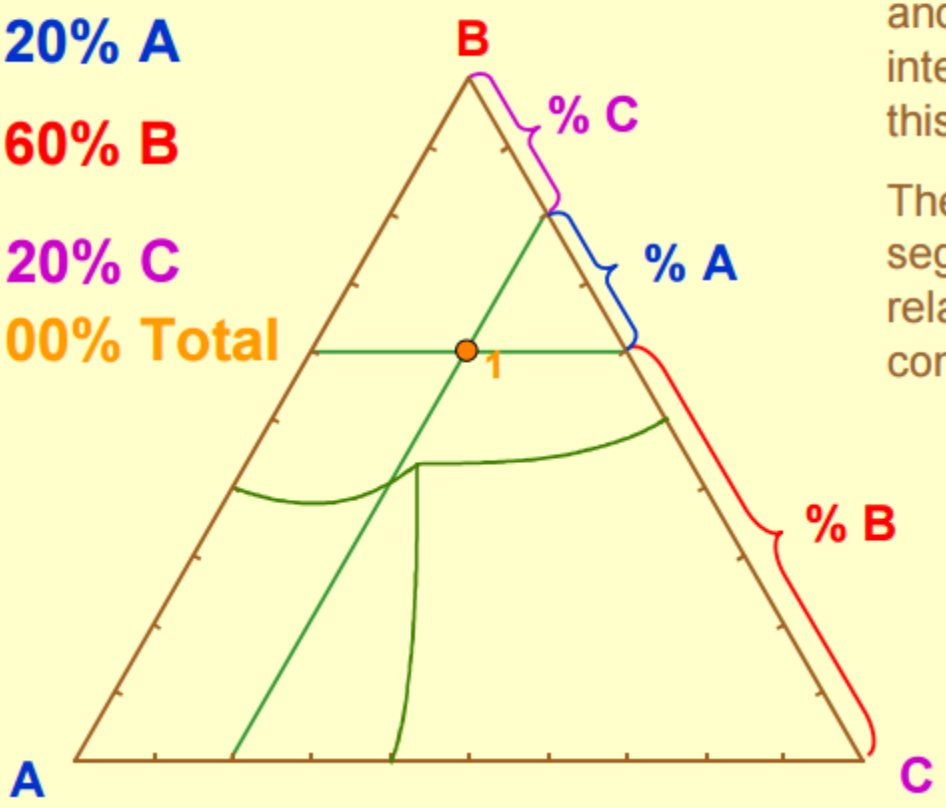

The two lines are parallel to the **AB** and **AC** sides of the triangle and intersect along the **BC** side, dividing this side into three line segments.

The lengths of the individual line segments are proportional to the relative amounts of the three components **A**, **B** and **C**.

Ternary Compositions

Determine the compositions of the points in the following table.

	% A	% B	%C
E			
1			
2			
e_3